Journal of Qassim University for Science
2024, *Vol 3* (Issue 2), pp. 93-137
Received: 12 September 2024
Revised: 5 October 2024
Accepted: 5 November 2024

JQUS

Calculating Gamow-Teller and Fermi Strength Function Using Two-Particle Two-Hole

Afnan Al-Shammari and Bassam Shehadeh
Department of Physics, Qassim University, Burydah, Qassim 51411, KSA.

Abstract

In this study, we investigated the transitions of all types of beta decays using the two-particle and two-hole techniques. Specifically, we calculated the binding energy for Fermi decay and Gamow-Teller transitions by applying this technique to several intermediate isotopes. This involved calculating the transition forces and matrix elements for both Gamow-Teller and Fermi. These calculations were crucial for determining the half-life values of these isotopes and comparing them with existing experimental values. Our results demonstrate a significant agreement between the theoretical and experimental outcomes. Hence, we obtain the reduced amplitudes and the log ft factor and the half-lives of the decay. Beta β^- and beta β^+/EC transitions from light to medium nuclei. The nuclei are ^{6}He, ^{18}Ne, ^{18}F, and ^{42}Sc.

1. Introduction

Beta-decay is a crucial process in nuclear physics, influencing several scientific disciplines, notably astrophysics and particle physics. The study of beta-decay provides valuable insights into the relationships between nuclear interactions and factors such as spin and isospin, along with other nuclear characteristics like mass, shape, and energy levels [1, 2]. In the context of astrophysics, β-decay is instrumental in the creation of neutron stars, which are significant in the synthesis of heavy elements within nature [3], by establishing the time frame for the rapid neutron-capture process through the half-life of β-decay. In the physics of particles, β-decay provided the initial experimental proof of parity violation [4] and has been used to confirm the Cabibbo–Kobayashi–Maskawa (CKM) matrix's unitarity [5].

The precise measurements of beta decay strength functions, and hence the decay half-lives, is a critical method for exploring physics Beyond the Standard Model (BSM). Such exploration could potentially reveal a new fundamental physics through beta decay in atomic nuclei. Moreover, the theoretical treatment of experimentally favored nuclei, in a framework that allows measuring uncertainties, remains complex. Despite these challenges, considerable progress has been made in recent decades towards the systematic development of internucleon interactions within a strong field theory framework. The medium-mass nuclei, often significant in BSM search, can now be approached from first principles, due to developments in the many-body theory and computational capabilities [6]. Yet, the impact of approximation strategies in ab initio calculations on crucial observables remains an area for further research.

With recent advancements in the measurement of nuclear β-decay half-lives facilitated by radioactive ion-beam facilities; a comprehensive compendium of experimental data is now accessible [7]. It is imperative to calculate the fundamental theoretical models and their abilities to reproduce the experimental outcomes and identify their strengths or weaknesses points in these models. This review highlights the current β-decay theory and the assessment of transition matrices stemming from the β-decay processes [8].

The two-particle, two-hole model provides an essential framework for describing nucleon correlations that are not captured by simpler single-particle models. These correlations arise when nucleons are excited from occupied states to unoccupied states (holes) or vice versa when additional nucleons are placed in an excited state. Key configurations include:

- **Two-particle excitations**: Two nucleons move from lower to higher energy levels, forming two particle-hole pairs.
- **Two-hole excitations**: The removal of two nucleons from an orbital leaves two vacancies (holes) in the nuclear shell.

These configurations are critical for understanding nuclear structure, particularly in beta decay, as weak interactions can induce transitions between nucleons. Two-particle and two-hole excitations can greatly affect transition probabilities and the shape of the strength function. Including two-particle and two-hole excitations provides a more accurate description of the energy distribution of final states in beta decay. The integration of the two-particle and two-hole states results in a more detailed and realistic energy distribution of the final states. This framework explains the mixing of configurations between the initial and final states, which is important for accurately modelling the beta decay process.

Several computational models have employed two-particle, two-hole excitations to study the beta-decay strength function. Civitarese et al. (1999) [9] explored beta decay using the quasiparticle-phonon model. This work found that collective excitations enhance the accuracy of the strength function, particularly at higher excitation energies. Bortignon et al. (2005) [10] applied the random phase approximation (RPA) to neutron-rich nuclei, emphasizing the importance of two-particle, two-hole correlations in reproducing decay rates. Danilo and Marcella (2022) [11] conducted shell-model calculations incorporating two-particles, two-hole excitations for medium-heavy nuclei. Their study demonstrated that higher-order configurations significantly influence decay rates and the shape of the strength function. In recent developments, the Monte Carlo shell model (MCSM) [12] has been increasingly employed for beta decay involving large nucleon numbers. In 2017 Tsunoda et al. demonstrated the MCSM ability to capture the effects of two-particle, two-hole excitations on decay rates, yielding highly accurate strength functions. Despite the progress in applying the theory of two-particles, two-hole, significant computational challenges remain. Techniques like the Monte Carlo shell model and the Kuo-Fineman model help address these complexities but demand substantial computational resources, particularly for heavy nuclei.

The two-particle, two-hole theory continues to refine our understanding of nuclear structure and weak interactions, enabling precise modelling of beta decay and contributing to further progress in nuclear physics and astrophysics. The Gamow-Teller decay for nuclear systems, starting from a nuclear Hamiltonian and electroweak currents, for ^{40}Ca and ^{56}Ni closed cores in the framework of the realistic Shell model. The effective shell- model Hamiltonian and decay operators are derived using many bodies perturbation theory [13]. The phenomenon of the quenching of the spin-isospin matrix elements has been extensively studied since the 80s of the last centuries, but in recent years there has been a renewed interest in his subject because of its possible implication in the neutrino less double-β decay.

Beta-decay strength function calculation using the two-particle, two-hole theory is carried out in most recent works via the SSRPA model [14]. This model incorporates energy density functions (EDFS) and the configuration of two-particle-two-hole states to enhance the accuracy of beta-decay calculations [14]. In the two-particle-two-hole model (SSRPA), Gamow-Teller (GT) states are shifted downward, significantly influencing the beta-decay process by increasing the beta-decay phase space while greatly reducing the half-life of beta decay in nuclei [14]. Incorporating the tensor factor into this model (SSRPA), further refines predictions of beta-decay half-lives by accurately reproducing excitation energies [14]. The two-particle-two-hole configurations and the tensor factor have been applied to various magic nuclei, demonstrating remarkable agreement with experimental results compared to other models [14]. In previous research conducted in ref. [15], the study utilized the one-particle, one-hole theory to investigate beta decay in intermediate elements. This approach focused on modelling beta decay for even/odd isotopes using specific isotopes ^{15}N , ^{15}O , ^{17}F , ^{41}S. These isotopes were deemed suitable for the one-particle, one-hole model; however, they do not apply to systems requiring a two-particle, two-hole framework.

To address this limitation, the current study adopts the two-particle, two-hole model to explore beta decay in isotopes classified as even/even and odd/odd isotopes. The isotopes utilized in this study include ^{6}He , ^{18}Ne , ^{18}F and ^{42}S. This shift to the two-particle, two-hole model allows for a more comprehensive understanding of beta decay processes, expanding beyond the limitations of the one-particle, one-hole framework. Two-particle and two-hole techniques simulate the effects of nuclear correlation. Studying all possible transitions using single-particle states confirms the experimental levels of the reference isotopes used in this study. This way the inaccuracy in determining the correct energy level is fixed by projecting the results onto the experimental nuclear level.

Our investigation shed the light on all types of beta decays underlying transitions, using the two-particle and two-hole techniques. This includes calculating the binding energy for Fermi decay and Gamow-Teller then calculating the transition matrix elements for both Gamow-Teller and Fermi. These calculations were crucial for determining the half-life values of these isotopes and comparing them with existing experimental values. Our results demonstrate a significant agreement between the theoretical and experimental outcomes. Hence, we obtain the reduced amplitudes and the log ft factor and the half-lives of the decay. Beta β^- and beta β^+/EC transitions from light to medium nuclei.

If we establish two-particle states to define the valence nucleons separate from the core, using a phenomenological potential that includes spin-orbit interaction but excludes residual interaction. The dynamics of particle-hole interactions are employed to obtain initial and final states, and the two-particle transition amplitudes for Fermi and Gamow-Teller transitions are calculated, leading to the determination of reduced amplitudes, *logft* values, and half-lives of decays. The study examines β-decay in both beta β^- and beta β^+/EC transition across a range of light to medium nuclei, including ^{6}He, ^{18}Ne, ^{18}F, and ^{42}Sc. The conclusions and further research suggestions are included at the end of the work.

2. Theoretical background

2.1. Theory of nuclear β-decay

In the nuclear scale, theβ^-decay is written as

$$ {}^{A}_{Z}\mathrm{X}_{N} \rightarrow {}_{Z+1}^{\;\;\;A}\mathrm{Y}_{N-1} + e^- + \bar{\nu}_e\ . \tag{1}$$

The nuclear β^+ decay is:

$$ {}^{A}_{Z}\mathrm{X}_{N} \rightarrow {}_{Z-1}^{\;\;\;A}\mathrm{Y}_{N+1} + e^+ + \nu_e\ . \tag{2}$$

Finally, nuclear EC reads:

$$ {}^{A}_{Z}\mathrm{X}_{N} + e^- \rightarrow {}_{Z-1}^{\;\;\;A}\mathrm{Y}_{N+1} + e^+ + \ \bar{\nu}_e\ . \tag{3}$$

In the three processes, Shown the parent nucleus ^{A}X and the daughter nucleus ^{A}Y are isobars, i.e. both have the same mass number A. This process has a coupling constant G_F which is not fundamental. It involves two fundamental vertices of weak coupling g_W. The strength of weak interaction is measured in muon decay, shown in fig. (1), where $q^2 < m_\mu C^2$ =106 MeV. Thus, the W-boson propagator in the natural unit can be written as:

$$\frac{-i\left(g_{m\mu} - q_\mu q_v/m_w^2\right)}{q^2 - m_w^2} \approx \frac{i g_{m\mu}}{m_w^2}\ .$$

In muon decay, this becomes g_w^2/m_w^2. Hence, the weak coupling g_W can be related to $G_F$using [16].

$$\frac{G_F}{\sqrt{2}} = \frac{g_w^2}{8\left(m_\mu C^2\right)^2}. \tag{4}$$

This is valid for a large mass of W-boson and small energy $q^2$of β-decay, i.e. $q^2 \ll (m_w C^2)^2$. In the case of $q^2 \geq (m_w C^2)^2$, the weak interaction is more probable than electromagnetic force. In other words, the weak interaction is only weak because of the large W-boson mass($m_w = 80.403 \pm 0.029\mathrm{GeV}/C^2$). For muon decay $G_F = 1.16639(1) \times 10^{-5}\mathrm{GeV}^{-2}$[16].

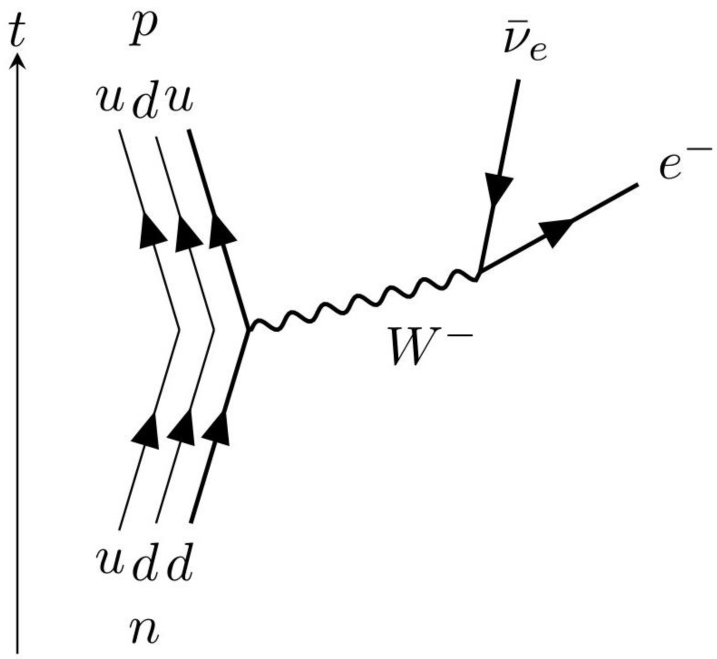

Figure 1: Feynman diagram depicts the weak muon decay. The W-boson propagator carries momentum q, where $q^2 \ll (m_w C^2)^2$, for precise measurements of the weak coupling g_W.

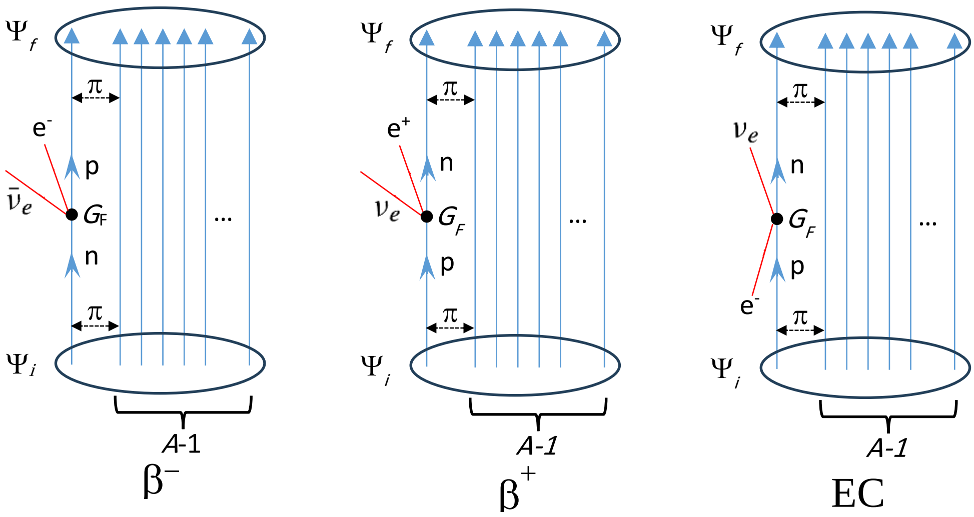

Figure 2: Nuclear β^- , β^+, and EC decay in the impulse approximation. In this picture only one nucleon contributes in the β decay process whereas the remaining $A-1$ nucleons are spectators. The initial and final states Ψ_i and Ψ_f are the intial and final nuclear states of a strongly interacting A-body wave function. At the weak-interaction vertices the antilepton lines are drawn as going backwards in time. The strength of the pointlike effective weak interaction vertex is given by the Fermi constant G_F.

2.2 Half-lives, Reduced transition probabilities, and ft values

Half-life represented by $t_{\frac{1}{2}}$ is computed from transition probability T_{fi},

$$t_{\frac{1}{2}} = \frac{ln2}{T_{fi}}, \tag{5}$$

T_{fi} is calculated Fermi golden rule of time-dependent perturbation theory to get [17]

$$t_{\frac{1}{2}} = \frac{\kappa}{f_0(B_F + B_{GT})}, \tag{6}$$

where κ (kappa) is constant [18]

$$\kappa = \frac{2\pi\hbar^7 ln2}{m_e^5 c^4 G_F^2} = 6147s, \tag{7}$$

f_0 is the Lepton kinematics phase space integral, and B_F and B_{GT} are the Fermi and Gamwo-Teller reduced transition probabilities that needed to be calculated, respectively. They can be broken up into factors [8],

$$B_F = \frac{g_V^2}{2J_i+1}\left|\mathcal{M}_F\right|^2, \tag{8}$$

And

$$B_{GT} = \frac{g_A^2}{2J_i+1}\left|\mathcal{M}_{GT}\right|^2, \tag{9}$$

where J_i is the nuclear total initial angular momentum (nuclear spin). g_A and g_v are coupling constants for axial current and vector current, respectively [19]. $\mathcal{M}_F$ and $\mathcal{M}_{GT}$ are the interaction amplitudes The quantity $f_0 t_{\frac{1}{2}}$ represents the allowed β-decay transitions. In [17] it has been called the reduced half-life or comparative half-life. The vector coupling constant $g_V = 1.0$. Its value is determined by conserved current $j^\mu = \frac{1}{2}\bar{\psi}\gamma^\mu\psi$ [8]. The factor $g_A = 1.25$ is the axial vector coupling constant of the weak interaction conserved axial vector current $j_A^\mu = \frac{1}{2}\bar{\psi}\gamma^\mu\gamma^5\psi$. Vectors have parity properties, $\vec{V}(-\vec{r}) = -\vec{V}(\vec{r})$ under space inversion. On the other hand, axial vectors $\vec{A}$ are invariant under space inversion,

$$\vec{A}(-\vec{r}) = +\vec{A}(\vec{r}).$$

For lepton current the violation of parity conservation is maximal, and the weak interaction amplitude for the leptonic contribution contains the combination $V - A$ in equal division. This holds at the quark level of the hadrons [16].

The hadronic current:

$$j \propto V - \left(\frac{g_A}{g_V}\right) A = V - (1.25A)\ . \tag{10}$$

Thus the $V - A$ current is proportional to

$$V - A \propto \bar{\psi}\gamma^{\mu}(1 - \gamma^{5})\psi. \tag{11}$$

The minus sign is an indication of the left-handedness of the Leptons involved in the weak interactions. Since the ft value is large can be suppressed by logarithm,

$$\log ft = log_{10}\left(f_0 t_{\frac{1}{2}}[s]\right). \tag{12}$$

2.3 Wigner –Eckart theorem

Assume $T_q^{(k)}$ is a spherical tensor operator (such as angular momentum operators) that acts on an angular momentum basis $|jm\rangle$. The transition amplitude resulting from this tensor operator is detailed in references [20,21]

$$\langle \xi_f; j_f m_f \left| T_q^{(k)} \right| \xi_i; j_i m_i \rangle = M\delta_{m_f m_i + q}\ ,$$

$m_f = m_i + q$ unless $M = 0$. This is the Wigner-Eckart theorem. According to this theorem, the matrix elements of tensor operators concerning angular momentum eigenstates satisfy [21]:

$$\langle \xi' : j'm' \left| T_q^{(k)} \right| \xi; jm \rangle = \langle jm; kq | jk; j'm' \rangle \frac{\langle \xi' j' \| T^{(k)} \| \xi j \rangle}{\sqrt{2j+1}}, \tag{13}$$

Where the double-bar matrix element is independent of m, m', and q. The amplitude in the left-hand side represents the transition rom $|\xi; jm\rangle$ to $|\xi'; j'm'\rangle$. Before we present proof of this theorem, let us look at its significance. First, we see that the matrix element is written as the product of two factors. The first factor is a Clebsch-Gorden coefficient for adding j and k to get j'. It depends only on geometry, which is on the way that the system is oriented concerning the z-axis. There is no reference whatsoever to the nature of the tensor operator. The second factor does depend on the dynamics;

for instance, ξ may stand for the radial quantum number, and its evaluation may involve. To evaluate $\langle \xi' : j'm' \left| T_q^{(k)} \right| \xi; jm \rangle$ with various combinations of m', m and q'it is sufficient to know just one of these combinations; all others can be geometrically related because they are proportional to the Clebsch-Gordan coefficients, which are predetermined and well-known. The common proportionality factor is $\langle \xi' j' \| T^{(k)} \| \xi j \rangle$, which does not refer whatsoever to the geometric features. There are different conventions for the reduced matrix elements. One convention includes an additional phase and normalization. The factor with the aid of the $6j$ symbol [20,22]

$$\langle \xi' : j'm' \left| T_q^{(k)} \right| \xi; jm \rangle = (-1)^{j-m} \begin{Bmatrix} j' & k & j \\ -m' & q & m \end{Bmatrix} \langle \xi' j' \| T^{(k)} \| \xi j \rangle \; . \tag{14}$$

2.4 Gamow –Teller and Fermi matrix element

In the beginning, let us review the scales of β-decay we need for evaluating the transition matrices. They are as follows:

1. Nuclear scale, where the β^--decay is due to the following nuclear decay:

$$^{A}_{Z}\mathrm{X}_N + e^- \rightarrow {}_{Z-1}^{\;\;A}\mathrm{Y}_{N+1} + e^+ + \bar{\nu}_e \; , \tag{15}$$

2. Quark scale: According to the standard model the β^--decay is attributed to the weak flavor symmetry down d and up u quarks, according to

$$u \rightarrow d + e + \bar{\nu}_e \; , \tag{16}$$

3. Nucleon scale: The β^--decay is due to the decay of a free (or quasi-free) neutron,

$$n \rightarrow p + e + \nu_e \; . \tag{17}$$

For nucleon scale β^--decay, we denote the proton using index *a* or *f*, and the neutron using index b or *i*. Whereas for β^+-decay, we denote the neutron using index *a* or *f*, and the proton using index *b* or *i*.

Fermi matrix element $\mathcal{M}_F$ [23] and Gamow-Teller (GT) matrix element $\mathcal{M}_{GT}$ [24] are the most important values that need to be calculated using the initial and final nuclear wave function which carries the nuclear structure information. Fermi operator is just the unit operator $\hat{1}$. GT operator is the Pauli spin operator $\hat{\sigma}$.

The Gamow-Teller and Fermi can be written as [8]:

$$\mathcal{M}_F = \langle \xi_f J_f \| \hat{1} \| \xi_i J_i \rangle = \delta_{J_i J_f} \sum_{a.b} \mathcal{M}_F(fi) \left\langle \xi_f J_f \left\| \left[c_f^\dagger \tilde{c}_i \right]_{\Delta J=0} \right\| \xi_i J_i \right\rangle, \tag{18}$$

and

$$\mathcal{M}_{GT} = \langle \xi_f J_f \| \hat{\sigma} \| \xi_i J_i \rangle = \sum_{a.b} \mathcal{M}_{GT}(fi) \left\langle \xi_f J_f \left\| \left[c_f^\dagger \tilde{c}_i \right]_{\Delta J=1} \right\| \xi_i J_i \right\rangle \ , \tag{19}$$

Where $M_{GT}(fi)$ and $M_F(fi)$ are the single–particle matrix for GT and Fermi respectively. They can be written as [20,22]

$$\begin{aligned} \mathcal{M}_F(fi) &= \langle f \| \hat{1} \| i \rangle = \delta_{fij_f} = \langle n_f l_f j_f \| \hat{1} \| n_i l_i j_i \rangle, \\ &= \delta_{n_f n_i} \delta_{l_f l_i} \delta_{j_f j_i} \hat{j}_f . \end{aligned} \tag{20}$$

$$\mathcal{M}_{GT}(fi) = \frac{1}{\sqrt{3}} \langle f \| \hat{\sigma} \| i \rangle = \frac{1}{\sqrt{3}} \langle n_f l_f j_f \| \hat{\sigma} \| n_i l_i j_i \rangle, \tag{21}$$

$$= \frac{1}{\sqrt{3}} \sqrt{\frac{3}{2}} \times 2 \delta_{n_f n_i} \delta_{l_f l_i} \delta_{j_f j_i} \hat{j}_f \hat{j}_i \ (-1)^{l_f + l_i + \frac{3}{2}} \begin{Bmatrix} \frac{1}{2} & \frac{1}{2} & 1 \\ j_f & j_i & l_f \end{Bmatrix},$$

$$= \sqrt{2}\ \delta_{n_f n_i} \delta_{l_f l_i} \delta_{j_f j_i} \hat{j}_f \hat{j}_i \ (-1)^{l_f + l_i + \frac{3}{2}} \begin{Bmatrix} \frac{1}{2} & \frac{1}{2} & 1 \\ j_f & j_i & l_f \end{Bmatrix} .$$

2.5 Phase-space factors

The half-life contains the integrated leptonic phase space which is called a phase space factor f_0. Some references call it Fermi integral. For $\beta^\pm$ -decay, the phase-space factors are [7]

$$f_0 = \int_0^{E_0} F_0(\mp Z_f \,.\, \varepsilon) p \varepsilon (E_0 - \varepsilon)^2 d\varepsilon, \tag{22}$$

F_0 is the Fermi function. ε is the energy ratio given by:

$$\varepsilon = \frac{E_e}{m_e c^2}, \tag{23}$$

where E_0 is the total energy of the emitted electron or positron. E_0 denotes the nuclear energy difference:

$$E_0 = \frac{E_i - E_f}{m_e c^2}, \tag{24}$$

where E_i and E_f are the initial and final energy, respectively, for the nuclear state. The momentum is given by:

$$p = \sqrt{\varepsilon^2 - 1}\,, \tag{25}$$

For electron capture the phase-space factor is [7]:

$$f_0^{(EC)} = 2\pi(\alpha Z_i)^3(\varepsilon_0 + E_0)^2, \tag{26}$$

where:

$$\varepsilon_0 = \frac{m_e c^2 - B}{m_e c^2} \approx 1 - \frac{1}{2}(\alpha Z_i)^2, \tag{27}$$

where

$$\alpha = \frac{e^2/4\pi\epsilon_0}{\hbar c} = \frac{1}{137}. \tag{28}$$

We can expand the phase-space factor [7,25]:

$$f_0^{(\pm)} \approx \frac{1}{30}(E_0^5 - 10E_0^2 + 15E_0 - 6)F_0^{(PR)(\pm)}(\mp Z_f)\,. \tag{29}$$

2.6 *β*-decay *Q*-Values

The Q-values for any nuclear reaction or decay are given by:

$$Q = K_f + K_i = E_i - E_f\,, \tag{30}$$

Using eq. (24), For β^--decay we have

$$E_0 = \frac{Q_{\beta^-} + m_e c^2}{m_e c^2}, \tag{31}$$

For β^+-decay we have

$$E_0 = \frac{Q_{\beta^+} + m_e c^2}{m_e c^2}, \tag{32}$$

Finally, for EC

$$E_0 = \frac{Q_{EC} - m_e c^2}{m_e c^2}, \tag{33}$$

The Q-values for all decay are listed in [7]. The table of nuclides and represent the endpoint energy of the decay. The decay half-life can be calculated directly once the one-body transition densities.

$$\langle \xi_f J_f \| [c_a^\dagger \tilde{c}_b] \| \xi_i J_i \rangle. \tag{34}$$

2.7 Classification of β-decay

1. Super allowed transitions

This takes place for light nuclei such as $^3H, ^{14}C, ^{15}C, \cdots$ where all protons and final neutrons are at the Fermi level, result in an overlap in the initial and final nuclear wave function. This means that the transitions are of the SP-type and yield the maximum value of the F and GT matrix elements.

2. l forbidden allowed transitions

This type occurs in cases where a simple (SP) transition in the mean-field shell-model picture, is forbidden by $\Delta l = 0$. This means the forbiddingness is due to a single configuration approximate for ψ_f and ψ_i. using a configuration mixing based on the finite value for $\log ft$ is usually below 5 due to the lack of strength in the configuration mixing [26].

3. Unfavorable allowed transitions

Such transformations do not belong to either of the two types discussed above. They are allowed SP transitions in that there is no (l) forbidding. However, the SP transitions are suppressed in ψ_f and ψ_i due to the residual interaction.

Table 1: Classification of β-decay transition [27]

Types of β-decay	$log\, ft$
Unfavorable allowed	3.8-6.7
Super allowed	2.9-3.7
forbidden allowed (l)	≥ 5.0
1st -forbidden unique	8-10
1st -forbidden non-unique	6-9
2nd – forbidden	11-13
3rd – forbidden	17-19

2.8 Operators and Their Matrix Elements

For a one-body spherical tensor operator$\hat{T}_{LM_L}$, one can derive the following formula [28]

$$T_{LM_L} = \sum_{\alpha\beta} \langle\alpha|\hat{T}_{LM_L}|\beta\rangle c_\alpha^\dagger c_\beta = \hat{L}^{-1} \sum_{ab} \left(a\|\hat{\boldsymbol{T}}_L\|b\right) [c_a^\dagger \tilde{c}_b]_{LM_L} . \quad (35)$$

Here

$$\tilde{c}_\alpha \equiv (-1)^{j_a+m_\alpha} c_{-\alpha}; \qquad c_{-\alpha} = c_{a,-m_\alpha},$$

is an annihilation operator with the proper behavior of a spherical tensor of rankj_a. The matrix element $\langle\alpha|\hat{T}_{LM_L}|\beta\rangle$ is the single-particle transition matrix, whereas the matrix element$(a\|\hat{\boldsymbol{T}}_L\|b)$ is the reduced single-particle transition matrix. Those matrix elements offer information related to the characteristics of the given one-body operator. They completely characterize the operator; they have nothing to do with the many-body characteristics of the nuclear structure. The many-nucleon structure is probed by the last factor T_{LM_L}, namely $[c_a^\dagger \tilde{c}_b]_{LM_L}$ which contains the particle creation and annihilation operators. One can imagine that the one-body operator probes the nucleus by scattering particles from one single-particle orbital to another. To each scattering it attaches an amplitude, the single-particle matrix element, characterizing the scattering properties of the operator itself. The reduced matrix element of the electromagnetic operator $\mathcal{O}_{\lambda\mu}$ is:

$$\left(\Psi_f J_f\|\mathcal{O}_{\lambda\mu}\|\Psi_i J_i\right) = \hat{\mu}^{-1} \sum_{a_f b_i} (a_f\|\mathcal{O}_{\lambda\mu}\|b_i)(\Psi_f J_f\|[c_{a_f}^\dagger \tilde{c}_{b_i}]_\lambda\|\Psi_i J_i) , \quad (36)$$

The reduced single-particle matrix element $(a_f\|\mathcal{O}_{\lambda\mu}\|b_i)$ can be easily written for any transitions.

2.9 Electromagnetic Transitions in Two-Particle and Two-Hole Nuclei

Let us start from the two-particle nuclei state given in eq (1) as the initial state and the final states can be written as

$$|\Psi_i\rangle = |a_i b_i; J_i \ M_i\rangle = \mathcal{N}_{a_i b_i}(J_i) \left[c_{a_i}^\dagger c_{b_i}^\dagger\right]_{J_i M_i} |CORE\rangle, \quad (37)$$

$$|\Psi_f\rangle = |a_f b_f; J_f \ M_i\rangle = \mathcal{N}_{a_f b_f}(J_f) \left[c_{a_f}^\dagger c_{b_f}^\dagger\right]_{J_f M_f} |CORE\rangle, \quad (38)$$

here a_i, b_i, a_f, and b_f are the initial proton-neutron, proton-proton, neutron-neutron, initial and final particles. The normalization factor is given in eq (14) Using the Wigner–Eckart theorem eq (14) we can write the reduced one-body transition density as symbol [20,22].

$$\begin{aligned}
\left(\Psi_f \left\| \left[c_a^\dagger \tilde{c}_b\right]_L \right\| \Psi_i\right) &= (-1)^{J_f-M_f} \begin{pmatrix} J_f & L & J_i \\ -M_f & M_L & M_i \end{pmatrix}^{-1} \mathcal{N}_{a_f b_f}(J_f) \mathcal{N}_{a_i b_i}(J_i) \\
& \left\langle CORE \left| \left[c_{a_f}^\dagger c_{b_f}^\dagger\right]^\dagger_{J_f M_f} \left[c_a^\dagger \tilde{c}_b\right]_{L M_L} \left[c_{a_i}^\dagger c_{b_i}^\dagger\right]_{J_i M_i} \right| CORE \right\rangle, \\
&= (-1)^{J_f-M_f} \begin{pmatrix} J_f & L & J_i \\ -M_f & M_L & M_i \end{pmatrix}^{-1} \mathcal{N}_{a_f b_f}(J_f) \mathcal{N}_{a_i b_i}(J_i) \\
& \sum_{m_{\alpha_f} m_{\beta_f} m_\alpha m_\beta m_{\alpha_i} m_{\beta_i}} \langle j_{a_f} m_{\alpha_f} j_{b_f} m_{\beta_f} | J_f M_f \rangle \langle j_a m_\alpha j_b m_\beta | L M_L \rangle \times \\
& \langle j_{a_i} m_{\alpha_i} j_{b_i} m_{\beta_i} | J_i M_i \rangle \left\langle CORE \left| c_{\beta_f} c_{\alpha_f} c_\alpha^\dagger \tilde{c}_\beta c_{\alpha_i}^\dagger c_{\beta_i}^\dagger \right| CORE \right\rangle.
\end{aligned}$$

Performing contractions in the core expectation value, we have three possible contractions permuted to span over four possible terms [29]. For example, one of them

$$c_{\beta_f} c_{\alpha_f} c_\alpha^\dagger \tilde{c}_\beta c_{\alpha_i}^\dagger c_{\beta_i}^\dagger = \delta_{\beta_i \beta_f} \delta_{\alpha_f \alpha} \delta_{-\beta \alpha_i}$$

All possible contractions for the core expectation value give:

$$\left\langle CORE \left| c_{\beta_f} c_{\alpha_f} c_\alpha^\dagger \tilde{c}_\beta c_{\alpha_i}^\dagger c_{\beta_i}^\dagger \right| CORE \right\rangle = (-1)^{j_b+m_\beta} \begin{pmatrix} \delta_{\beta_i \beta_f} \delta_{\alpha_f \alpha} \delta_{-\beta \alpha_i} - \\ \delta_{\beta_f \alpha_i} \delta_{\alpha_f \alpha} \delta_{-\beta \beta_i} + \\ \delta_{\beta_f \alpha} \delta_{\alpha_i \alpha_f} \delta_{-\beta \beta_i} - \\ \delta_{\beta_f \alpha} \delta_{\beta_i \alpha_f} \delta_{-\beta \alpha_i} \end{pmatrix}.$$

Thus, the reduced one-body transition density becomes:

$$\left(\Psi_f \left\| \left[c_a^\dagger \tilde{c}_b\right]_L \right\| \Psi_i\right) = (-1)^{J_f-M_f} \begin{pmatrix} J_f & L & J_i \\ -M_f & M_L & M_i \end{pmatrix}^{-1} \mathcal{N}_{a_f b_f}(J_f) \mathcal{N}_{a_i b_i}(J_i) \times$$
$$\begin{bmatrix} \sum_{m_{\alpha_f} m_{\beta_f} m_{\alpha_i}} (-1)^{j_b - m_{\alpha_i}} \langle j_{a_f} m_{\alpha_f} j_{b_f} m_{\beta_f} | J_f M_f \rangle \langle j_a m_{\alpha_f} j_b - m_{\alpha_i} | L M_L \rangle \langle j_{a_i} m_{\alpha_i} j_{b_i} m_{\beta_f} | J_i M_i \rangle - \\ \sum_{m_{\alpha_f} m_{\beta_f} m_{\beta_i}} (-1)^{j_b - m_{\beta_i}} \langle j_{a_f} m_{\alpha_f} j_{b_f} m_{\beta_f} | J_f M_f \rangle \langle j_a m_{\alpha_f} j_b - m_{\beta_i} | L M_L \rangle \langle j_{a_i} m_{\beta_f} j_{b_i} m_{\beta_i} | J_i M_i \rangle + \\ \sum_{m_{\alpha_f} m_{\beta_f} m_{\beta_i}} (-1)^{j_b - m_{\beta_i}} \langle j_{a_f} m_{\alpha_f} j_{b_f} m_{\beta_f} | J_f M_f \rangle \langle j_a m_{\beta_f} j_b - m_{\beta_i} | L M_L \rangle \langle j_{a_i} m_{\alpha_f} j_{b_i} m_{\beta_i} | J_i M_i \rangle - \\ \sum_{m_{\alpha_f} m_{\beta_f} m_{\alpha_i}} (-1)^{j_b - m_{\alpha_i}} \langle j_{a_f} m_{\alpha_f} j_{b_f} m_{\beta_f} | J_f M_f \rangle \langle j_a m_{\beta_f} j_b - m_{\alpha_i} | L M_L \rangle \langle j_{a_i} m_{\alpha_i} j_{b_i} m_{\alpha_f} | J_i M_i \rangle \end{bmatrix}.$$

The Clebsch-Gordan coefficients are converted into *3j* symbols. The three *3j* symbols can be summed into a *3j* symbol times a *6j* symbol [30].

$$\sum_{m_{\alpha_f} m_{\beta_f} m_{\alpha_i}} \langle j_{a_f} m_{\alpha_f} j_{b_f} m_{\beta_f} | J_f M_f \rangle \langle j_a m_{\alpha_f} j_b - m_{\alpha_i} | L M_L \rangle \langle j_{a_i} m_{\alpha_i} j_{b_i} m_{\beta_f} | J_i M_i \rangle =$$

$$\delta_{b_i b_f} \delta_{a a_f} \delta_{b a_i} \widehat{L} \widehat{J_i} \widehat{J_f} (-1)^{j_{a_f} + j_{b_f} - M_i - M_L} \begin{pmatrix} J_f & J_i & L \\ -M_f & M_i & M_L \end{pmatrix} \begin{Bmatrix} J_f & J_i & L \\ j_{a_i} & j_{a_f} & j_{b_f} \end{Bmatrix},$$

Make use of eq. (36) we reach to the reduced matrix element for two-proton and two-neutron nuclei:

$$(a_f b_f; J_f \| \mathcal{O}_{\lambda\mu} \| a_i b_i; J_i) = \widehat{J}_i \widehat{J_f} \mathcal{N}_{a_i b_i}(J_i) \mathcal{N}_{a_f b_f}(J_f) \times$$
$$\left[\begin{array}{r} \delta_{b_i b_f} (-1)^{j_{a_f} + j_{b_f} + J_i + \mu} \begin{Bmatrix} J_f & J_i & \mu \\ j_{a_i} & j_{a_f} & j_{b_f} \end{Bmatrix} (a_f \| \mathcal{O}_{\lambda\mu} \| a_i) + \\ \delta_{a_i b_f} (-1)^{j_{a_f} + j_{b_i} + \mu} \begin{Bmatrix} J_f & J_i & \mu \\ j_{b_i} & j_{a_f} & j_{b_f} \end{Bmatrix} (a_f \| \mathcal{O}_{\lambda\mu} \| b_i) + \\ \delta_{a_i a_f} (-1)^{j_{a_i} + j_{b_i} + J_f + \mu} \begin{Bmatrix} J_f & J_i & \mu \\ j_{b_i} & j_{b_f} & j_{a_f} \end{Bmatrix} (b_f \| \mathcal{O}_{\lambda\mu} \| b_i) + \\ \delta_{b_i a_f} (-1)^{J_f + J_i + \mu + 1} \begin{Bmatrix} J_f & J_i & \mu \\ j_{a_i} & j_{b_f} & j_{a_f} \end{Bmatrix} (b_f \| \mathcal{O}_{\lambda\mu} \| a_i) \end{array} \right]. \tag{39}$$

This equation is the basis for calculating the decay amplitude of the two-particle beta decay.

2.10 Nuclei with two-holes and two-particles

By producing two particles in the suitable vacuum state, two particles can be described as two-particle nuclei inside the notation of occupation number (core), similarly the two-hole nuclei are also described using occupation number representation by creating two holes into a vacuum. The procedure we follow to create the two-particles, or two-holes states is similar to the one for one–particle and one–hole nuclei [8]. A coupling of rotational momentum is required to explain the two-holes or two-particles nuclear states.

2.10.1 Two–Particle Nuclei

We have two nuclear outside the core, the nuclear state of two nuclei a and b is written as in [8].

We can express the wave function in this case of two-like nucleons a and b outside the core as

$$|a, b; JM\rangle = \mathcal{N}_{ab}(J) \sum_{m_\alpha m_\beta} \langle j_\alpha m_\alpha j_\alpha \beta_\alpha | JM \rangle c_\alpha^\dagger c_\beta^\dagger | CORE \rangle,$$

$$= \mathcal{N}_{ab}(J)\left[c_a^\dagger c_b^\dagger\right]_{JM}|CORE\rangle, \quad (40)$$

where

$$\left[c_a^\dagger c_b^\dagger\right]_{JM} = \sum_{m_\propto m_\beta} \langle j_\alpha m_\alpha j_\alpha \beta_\alpha | JM\rangle c_\alpha^\dagger c_\beta^\dagger. \quad (41)$$

The factor $\mathcal{N}_{ab}$ is the normalization factor [8]

$$\mathcal{N}_{ab}(J) = \sqrt{\frac{1+\delta_{ab}(-1)^J}{1+\delta_{ab}}}\ , \quad (42)$$

Both α and β are the quantum numbers, signify either proton or neutron orbitals. Two identical nucleons in their SP orbitals $\alpha = n_\alpha l_\alpha j_\alpha m_\alpha$, the normalization factor

$$\mathcal{N}_{ab}(J) = \begin{cases} 1 & \text{for } a \neq b, \\ 0 & \text{for } a = b \text{ } and \text{ } J \text{ is odd,} \\ \frac{1}{\sqrt{2}} & \text{for } a = b \text{ } and \text{ } J \text{ is even.} \end{cases} \quad (43)$$

Two particle nuclei are always even-even (or doubly even) nuclei. In case of neutron and proton outside the core the nuclear state has the from

$$|pn; JM\rangle = \left[c_a^\dagger c_b^\dagger\right]_{JM}|CORE\rangle(J) \sum_{m_\pi m_\nu} \langle j_p m_\pi j_n m_\nu | JM\rangle c_\pi^\dagger c_\nu^\dagger |CORE\rangle \quad (44)$$

where $\pi = (n_p l_p j_p m_\pi)$ and $\nu = (n_n l_n j_n m_\nu)$. Two-particle nuclei of this type are always odd-odd unusual-odd (doubly odd). Those who perform creation in (44) or (40) are always anti-commute. From symmetry properties of Clebsch-Gordan coefficients, the two particles state inversion relations [31]

$$|ba; JM\rangle = (-1)^{j_a + j_b + J + 1}|ab; JM\rangle, \quad (45)$$

$$|np; JM\rangle = (-1)^{j_b + j_n + J + 1}|pn; JM\rangle. \quad (46)$$

Accordingly, nuclei with the same mass number A (isobar), have comparable properties, this can be attributed to the fact that the nuclear force is charge independent. For example isobars ${}^{14}_{6}C_8$ and ${}^{14}_{8}O_6$ have identical properties. Another example is the $A = 6$ isobars ${}^{6}He$ and ${}^{6}Li$.

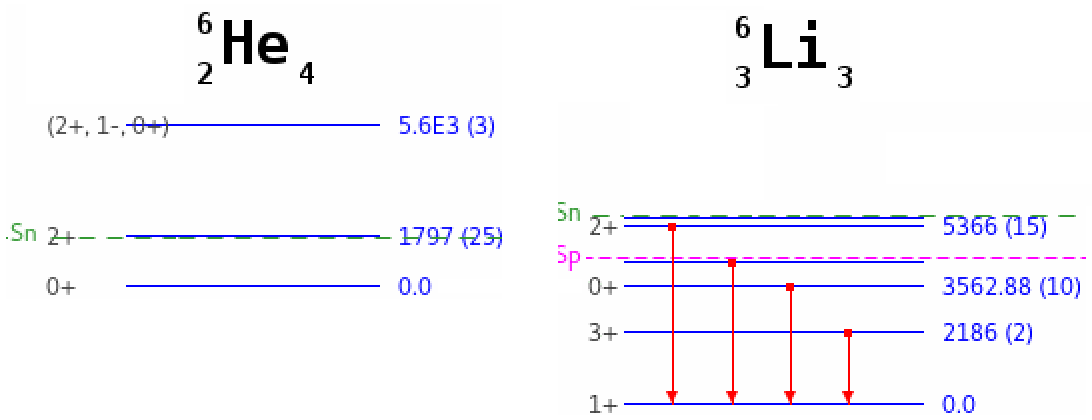

Figure 3: Experimental low-energy spectra of the two-particle nuclei ^{6}He and ^{6}Li. Energy levels (blue lines) are in keV. The Coulomb energy has been subtracted and the isospin quantum numbers of the relevant states are displayed. In ^{6}Li the 2^+ state at 5.366 MeV is unbound. The energy gab between the 2^+ and 0^+ states in ^{6}Li is about 1.8 MeV whereas for ^{4}He the energy gab is 1.79 MeV. Taken from International Atomic Energy Agency [32].

The ground state isospin is given by

$$T = \frac{|N-Z|}{2}. \tag{47}$$

Accordingly, $T(^6\mathrm{He}) = 1$ with $J^\pi = 0^+$for the ground state. Whereas $T(^6\mathrm{Li}) = 0$ with $J^\pi = 1^+$. Both isobars have the core contains only $0s_{\frac{1}{2}}$ thus

$$|CORE\rangle = |CORE(0s)\rangle_\pi \, |CORE(0s)\rangle_\nu \, .$$

The nuclear state for ^{6}He is thus

$$|^6\mathrm{He}, 0^+, 2^+\rangle = \frac{1}{\sqrt{2}} \left[c^\dagger_{\nu 0 p_{\frac{3}{2}}} \, c^\dagger_{\nu 0 p_{\frac{3}{2}}} \right]_{0^+, 2^+} |CORE\rangle \, , \tag{48}$$

The angular moment obeys the of triangular condition

$$\Delta(j_1 j_2 J) = |j_1 - j_2| \le J \le |j_1 + j_{2<}| \to 0 \le J \le 3, \tag{49}$$

Which means $J = \{0,1,2,3\}$. Hence,

$$|^6\mathrm{Li}, 0^+, 1^+, 2^+, 3^+\rangle = \frac{1}{\sqrt{2}} \left[c^\dagger_{\pi 0 p_{\frac{3}{2}}} c^\dagger_{\nu 0 p_{\frac{3}{2}}} \right]_{0^+, 1^+, 2^+, 3^+} |CORE\rangle. \tag{50}$$

We have some important isobars used to study GT strength function $^{14}_{6}\mathrm{C}_8$ and $^{14}_{8}\mathrm{O}_6$ innershell electrons can spend some times inside nucleus and thus there is ptobability for an excess proton capture the electron to become a neutron in an electronic capture process (EC) according to

$$ {}_{1}^{1}p + {}_{-1}^{0}e \rightarrow {}_{0}^{1}n + \nu_e. $$

2.10.2 Two-Hole Nuclei

The wave function of the two-hole nuclei is similar to those two-particle nuclei. For two proton holes or two neutron holes we have

$$ |a^{-1}b^{-1}; JM\rangle = \mathcal{N}_{ab}(J)\left[h_a^\dagger h_b^\dagger\right]|HF\rangle, \tag{51} $$

where $a^{-1}$and b^{-1}indicate holes for particles a and b, respectively. The normalization factor is given in eq. (43) [11]. It is worth noting that the energy level of the $|HF\rangle$ state versus the $|CORE\rangle$ state, compared to the Fermi energy $\mathcal{E}_F$ is as follow

$$ \mathcal{E}_{HF} \approx \mathcal{E}_F; \qquad \mathcal{E}_{CORE} < \mathcal{E}_F. \tag{52} $$

For example, in one-neutron one-proton hole nucleus, we have

$$ |p^{-1}n^{-1}; JM\rangle = \left[h_p^\dagger h_n^\dagger\right]|HF\rangle, \tag{53} $$

In case of two-neutron-hole or two-proton-hole nuclei. They are always even-even nuclei. whereas proton-neutron-hole nuclei are always odd-odd. The hole-creation operators $h_a^\dagger$ are anti-commute [33]. odd-odd. Also, there are symmetry properties of the Clebsch –Gordan coefficients, given by [34]

$$ |b^{-1}a^{-1}; JM\rangle = (-1)^{j_{a^{-1}}+j_{b^{-1}}+J+1}|a^{-1}b^{-1}; JM\rangle\,, \tag{54} $$

Thus

$$ |n^{-1}p^{-1}; JM\rangle = (-1)^{j_{p^{-1}}+j_{n^{-1}}+J+1}|p^{-1}n^{-1}; JM\rangle. \tag{55} $$

Again, the isobars with the neutron-proton-hole have similar nuclear properties [35].

An important example for EC process is

$$ {}_{20}^{38}\mathrm{Ca}_{18} \xrightarrow{EC} {}_{19}^{38}\mathrm{K}_{19}, \tag{56} $$

The nuclear state for ^{38}Ca and ^{38}K are

$$ |{}^{38}\mathrm{Ca}; 0^+, 2^+\rangle = \frac{1}{\sqrt{2}}\left[h^\dagger_{\nu 0d\frac{3}{2}} h^\dagger_{\nu 0d\frac{3}{2}}\right]_{0^+,2^+}|HF\rangle, \tag{57} $$

and

$$ |{}^{38}\mathrm{K}; 0^+, 1^+, 2^+, 3^+\rangle = \frac{1}{\sqrt{2}}\left[h^\dagger_{\pi 0d\frac{3}{2}} h^\dagger_{\nu 0d\frac{3}{2}}\right]_{0^+,1^+,2^+,3^+}|HF\rangle \tag{58} $$

3. Results and discussion

3.1 Electromagnetic transition in Two – Particle and Two – hole nuclei

Consider two-particle and two-hole nuclei. The initial and final states in the electromagnetic decay process are [36,37]

$$|\psi_i\rangle = |a_i\, b_i; JM\rangle = \mathcal{N}_{a_i b_i}(J_i)[c_{a_i}^{\dagger} c_{b_i}^{\dagger}]CORE\rangle, \tag{59}$$

$$|\psi_f\rangle = |a_f b_f; JM\rangle = \mathcal{N}_{a_f b_f}(J_f)\left[c_{a_f}^{\dagger} c_{b_f}^{\dagger}\right]|CORE\rangle, \tag{60}$$

$$|\psi_i\rangle = |a_i^{-1} b_i^{-1}; JM\rangle = \mathcal{N}_{a_i b_i}(J_i)[h_{a_i}^{\dagger} h_{b_i}^{\dagger}]|CORE\rangle, \tag{61}$$

$$|\psi_f\rangle = |a_f^{-1} b_f^{-1}; JM\rangle = \mathcal{N}_{a_f b_f}(J_f)\left[h_{a_f}^{\dagger} h_{b_f}^{\dagger}\right]|CORE\rangle, \tag{62}$$

where $c_{a_f}^{\dagger}, c_{b_f}^{\dagger}$ known as the creation final of the particle a and b. while $c_{a_i}^{\dagger}, c_{b_i}^{\dagger}$ known as the creation initial of the particle a and b.

These equations, with the aid of eq. (39), give the transition amplitude of two neutron states to neutron-proton particles due to the β^{-}-decay [36,37]

$$\begin{aligned} &\mathcal{M}_L^{(-)}(n_i n_i'; J_i \to p_f n_f; J_f) = \hat{L}\hat{J}_i\hat{J}_f \mathcal{N}_{n_i n_i'}(J_i) \times \\ &\left[\delta_{n_i' n_f}(-1)^{j_{p_f}+j_{n_f}+J_i+L}\begin{Bmatrix} J_i & J_f & L \\ j_{p_f} & j_{n_i} & j_{n_f}\end{Bmatrix}\mathcal{M}(p_f n_i) + \right. \\ &\left.\delta_{n_i n_f}(-1)^{j_{p_f}+j_{n_i'}+L}\begin{Bmatrix} J_i & J_f & L \\ j_{p_f} & j_{n_i'} & j_{n_f}\end{Bmatrix}\mathcal{M}(p_f n_i')\right], \end{aligned} \tag{63}$$

This equation gives the transition amplitude of neutron-proton state to two-proton state due to the β^{-}-decay

$$\begin{aligned} \mathcal{M}_L^{(-)}(p_i n_i; J_i \to p_f p_f'; J_f) &= \hat{L}\hat{J}_i\hat{J}_f \mathcal{N}_{p_f p_f'}(J_i) \\ &\times \left[\delta_{p_i p_f'}(-1)^{j_{p_f}+j_{n_i}+L}\begin{Bmatrix} J_i & J_f & L \\ j_{p_f} & j_{n_i} & j_{p_f'}\end{Bmatrix}\mathcal{M}(p_f n_i)\right. \\ &\left. + \delta_{p_i p_f}(-1)^{j_{p_f}+j_{n_i}+J_f+L}\begin{Bmatrix} J_i & J_f & L \\ j_{p_f'} & j_{n_i} & j_{p_f}\end{Bmatrix}\mathcal{M}(p_f' n_i)\right]. \end{aligned} \tag{64}$$

This equation gives the transition amplitude of two-proton state to neutron-proton particle state due to the β^+/EC-decay

$$\begin{aligned}
&\mathcal{M}_L^{(+)}(p_i p_i'; J_i \to p_f n_f; J_f) \\
&= \hat{L}\hat{j}_i\hat{j}_f \mathcal{N}_{p_i p_i'}(J_i) \\
&\times \left[\delta_{p_i p_f} (-1)^{j_{n_f}+j_{p_f}+J_f+L} \begin{Bmatrix} J_i & J_f & L \\ j_{n_f} & j_{p_i'} & j_{p_f} \end{Bmatrix} \mathcal{M}(p_i' n_f) \right. \\
&\left. + \delta_{p_i' p_f} (-1)^{j_{p_i}+j_{n_f}+J_i+J_f+L} \begin{Bmatrix} J_i & J_f & L \\ j_{n_f} & j_{p_i} & j_{p_f} \end{Bmatrix} \mathcal{M}(p_i n_f) \right].
\end{aligned} \tag{65}$$

This equation gives the transition amplitude of neutron-proton state to neutron-neutron particle state due to the β^+/EC-decay

$$\begin{aligned}
&\mathcal{M}_L^{(+)}(p_i n_i; J_i \to n_f n_f'; J_f) \\
&= \hat{L}\hat{j}_i\hat{j}_f \mathcal{N}_{n_f n_f'}(J_i) \\
&\times \left[\delta_{n_i n_f'} (-1)^{j_{p_i}+j_{n_i}+J_i+L} \begin{Bmatrix} J_i & J_f & L \\ j_{n_f} & j_{p_i} & j_{n_f'} \end{Bmatrix} \mathcal{M}(p_i n_f) \right. \\
&\left. + \delta_{n_i n_f} (-1)^{j_{p_i}+j_{n_f'}+J_i+J_f+L} \begin{Bmatrix} J_i & J_f & L \\ j_{n_f'} & j_{p_i} & j_{n_f} \end{Bmatrix} \mathcal{M}(p_i n_f') \right].
\end{aligned} \tag{66}$$

3.2 The β-decay of ^{6}He

The Beta-decay equation

$$ {}^{6}_{2}\mathrm{He}_4 \to {}^{6}_{3}\mathrm{Li}_3 + e^- + \bar{\nu}_e \ , \tag{67}$$

We can calculate the Q-value:

$$Q_{\beta^-} = 3.50521\ MeV. \tag{68}$$

The allowed transition

$$\nu 0p_{\frac{3}{2}} \nu 0p_{\frac{3}{2}}; J_i = 0^+ \ \to \pi 0p_{\frac{3}{2}} \nu 0p_{\frac{3}{2}}; J_f = 0^+, 1^+, 2^+, 3^+. \tag{69}$$

This is because the allowed total angular momentum quantum number states are

$$\left|\frac{3}{2} - \frac{3}{2}\right| \leq J_f \leq \left|\frac{3}{2} + \frac{3}{2}\right| \to J_f = 0^+, 1^+, 2^+, 3^+.$$

From fig. (3), the ground state of ^{6}Li is at $j = 1^+$. Thus, the initial state equation

$$|i\rangle = |{}^6\mathrm{He}, 0^+\rangle = \frac{1}{\sqrt{2}}\left[c^\dagger_{\nu 0p\frac{3}{2}} c^\dagger_{\nu 0p\frac{3}{2}}\right]_{0^+} |CORE\rangle\,, \tag{70}$$

The Final state equation

$$|f\rangle = |{}^6\mathrm{Li}, 1^+\rangle = \frac{1}{\sqrt{2}}\left[c^\dagger_{\pi 0p\frac{3}{2}} c^\dagger_{\nu 0p\frac{3}{2}}\right]_{1^+} |CORE\rangle\,. \tag{71}$$

This is a Gamow-Teller transition from neutron-neutron to proton-proton state. Thus, we use. eq (63) to evaluate the transition amplitude

$$\mathcal{M}_L^-\left(\nu 0p_{\frac{3}{2}}\nu 0p_{\frac{3}{2}}; J_i = 0^+ \to \pi 0p_{\frac{3}{2}}\nu 0p_{\frac{3}{2}}; J_f = 1^+\right) = \tag{72}$$

$$\hat{L}\sqrt{2\times 0+1}\,\sqrt{2\times 1+1}\mathcal{N}_{n_i n_i'}\left[(-1)^{\frac{3}{2}+\frac{3}{2}+0+L}\begin{Bmatrix} 0 & 1 & L \\ \frac{3}{2} & \frac{3}{2} & \frac{3}{2}\end{Bmatrix}\mathcal{M}_L\left(\pi 0p_{\frac{3}{2}}\nu 0p_{\frac{3}{2}}\right) + \right.$$

$$\left.(-1)^{\frac{3}{2}+\frac{3}{2}+L}\begin{Bmatrix} 0 & 1 & L \\ \frac{3}{2} & \frac{3}{2} & \frac{3}{2}\end{Bmatrix}\mathcal{M}_L\left(\pi 0p_{\frac{3}{2}}\nu 0p_{\frac{3}{2}}\right)\right]\,.$$

$\mathcal{M}_0^{(-)} = 0$ The transition is not allowed for Fermi ($L = 0$) due to the 6*j*-symbol. The right-hand side of eq. (72) of the decay transition of the Gamow-Teller

$$\sqrt{3}\,\frac{1}{2}\mathcal{N}_{n_i n_i'}2\mathcal{M}_{GT}\left(\pi 0p_{\frac{3}{2}}\nu 0p_{\frac{3}{2}}\right) = \sqrt{3}\,\frac{1}{2}\mathcal{N}_{n_i n_i'}2\;\frac{2\sqrt{5}}{3} = \frac{1}{\sqrt{2}}\frac{2\sqrt{5}}{3} = \sqrt{\frac{10}{3}}\;. \tag{73}$$

Using eq (9), the reduced amplitude for the Gamow-Teller transition is

$$B_{GT} = \frac{g_A^2}{2J_i+1}|\mathcal{M}_{GT}|^2 = \frac{(1.25)^2}{2\times 0+1}\left|\sqrt{\frac{10}{3}}\right|^2 = \frac{25}{16}\times\frac{10}{3} = \frac{125}{24}. \tag{74}$$

The half-life of the phase space factor becomes

$$f_0 t_{\frac{1}{2}} = \frac{\kappa}{(B_f + B_{GT})} = \frac{6147\ \mathrm{s}}{(0+5.208)} = 1180.3\ \mathrm{s}. \tag{75}$$

The *logft* value is thus

$$logft = \log(1180.3) = 3.07. \tag{76}$$

The experimental *logft* value is 2.9 [32]. The error in *logft* value is

$$error = \frac{3.07-2.9}{2.9}\times 100 = 5\%\;. \tag{77}$$

The calculated value using the two-particle and hole theory of β^--decay (67) agrees with to the experimental value up to 5%. The theory does offer good prediction for ^{6}He decay.

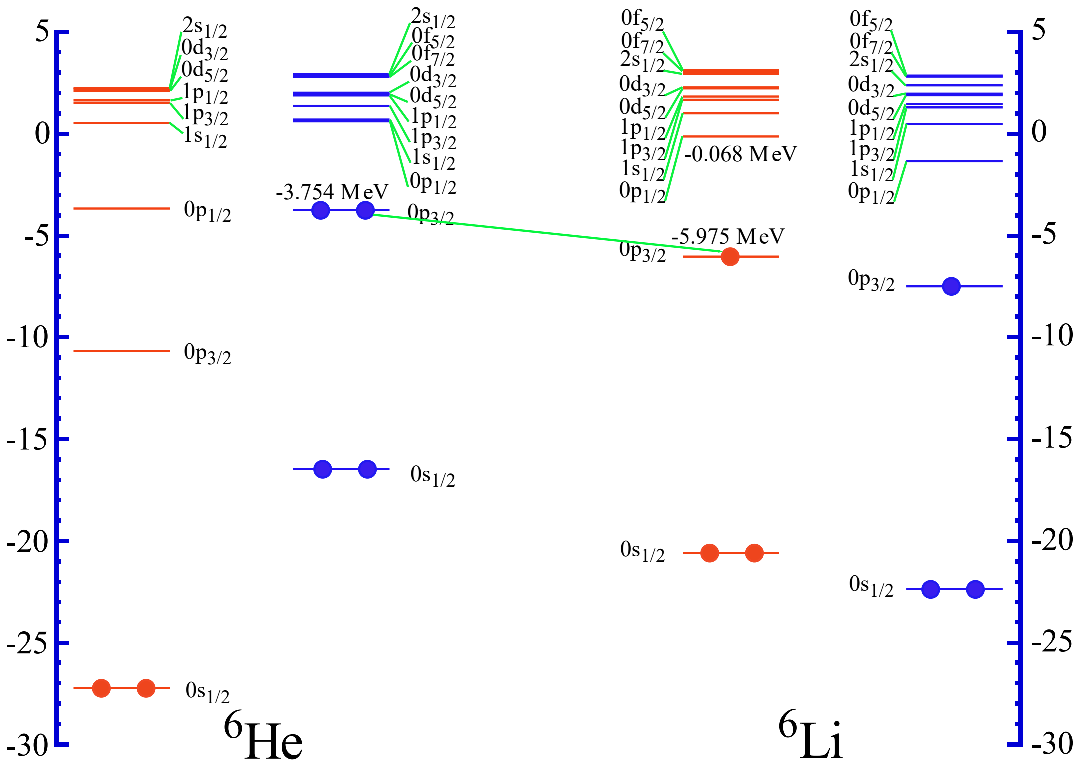

Figure 4: Single particle states for ^{6}He and ^{6}Li. The ground state of ^{6}Li is due to proton-neutron $\pi 0p_{\frac{3}{2}} \nu 0p_{\frac{3}{2}}$ pairing at j = 1$^+$. The first, second and third excited states of ^{6}Li in fig.3 is due to proton-neutron $\pi 0p_{\frac{3}{2}} \nu 0p_{\frac{3}{2}}$ pairing at j = 3$^+$,0$^+$, and 2$^+$, respectively.

The transition is summarized in fig. 5. The first, the second and the third excited states of ^{6}Li, shown in fig.3, is due to proton-neutron $\pi 0p_{\frac{3}{2}} \nu 0p_{\frac{3}{2}}$ pairing to j = 3$^+$,0$^+$, and 2$^+$, respectively. ^{6}Li cannot be created at first excited state 3$^+$ since it is not allowed by the 6j-symbol in eq. (63). The Q-value is not sufficient to create ^{6}Li at the second excited state 0$^+$ via the Fermi transition $(\nu 0p_{\frac{3}{2}} \nu 0p_{\frac{3}{2}}, 0^+)_{gs} \rightarrow (\pi 0p_{\frac{3}{2}} \nu 0p_{\frac{3}{2}}, 0^+)_{3.56\,\mathrm{MeV}}$. The formation of ^{6}Li at 2$^+$ state is inhibited by both energy and the 6j-symbol.

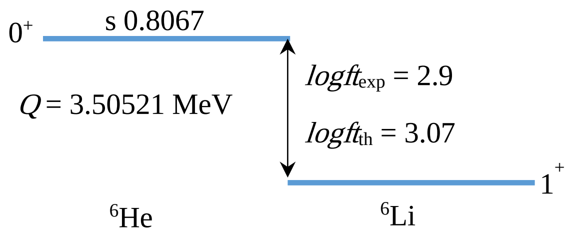

Figure 5: The transition chart of decay (67). The Q-value is not sufficient to create ^{6}Li at the second excited state 0^+ via the transition $(\nu 0p_{\frac{3}{2}} \nu 0p_{\frac{3}{2}}, 0^+)_{gs} \rightarrow (\pi 0p_{\frac{3}{2}} \nu 0p_{\frac{3}{2}}, 0^+)_{3.56\ \mathrm{MeV}}$. Also ^{6}Li cannot be created at first excited state 3^+ since it is not allowed by the 6j-symbol in eq (63). The formation of ^{6}Li at 2^+ state is inhibited by both energy and the 6j-symbol.

3.3 The β-decay of ^{18}Ne

The equation of ^{18}Ne decay for β^+ is

$$^{18}\mathrm{Ne} \rightarrow {}^{18}\mathrm{F} + \beta^+ + \nu_e\,, \tag{78}$$

whereas for EC, the equation of the decay is

$$^{18}\mathrm{Ne} + e \rightarrow {}^{18}\mathrm{F} + \nu_e\,, \tag{79}$$

with the Q-value [32]

$$Q_{EC} = 4.44\ \mathrm{MeV}. \tag{80}$$

From single particle states (see figs. 6-9) the decay involves transition of proton-proton to proton-neutron state. Thus, according to the theory of two-particle and two-hole, one need to use eq. (65) to calculate the transition amplitudes. We discuss all possible transitions as follow:

1- The first transition, depicted in fig.6, is

$$\left|i, \pi 0d_{\frac{5}{2}}\, \pi 0d_{\frac{5}{2}}, 0^+\right\rangle \rightarrow \left|f, \pi 0d_{\frac{5}{2}}\, \nu 0d_{\frac{5}{2}}\,, J_f = 0^+, 1^+, 2^+, 3^+, 4^+, 5^+\right\rangle.$$

The transition is shown in fig. (6). The nuclear spin for the ground state is $J_f = 1^+$and for the first excited state (1.04 MeV) $J_f = 0^+$. The transition from the initial state equation $|^{18}\mathrm{Ne}, 0^+\rangle_{gs}$ to $|^{18}\mathrm{F}, 1^+\rangle_{gs}$ is Gamow-Teller:

$$|i\rangle = |^{18}\mathrm{Ne}, 0^+\rangle_{gs} = \frac{1}{\sqrt{2}}\left[c^\dagger_{\pi 0d_{\frac{5}{2}}} c^\dagger_{\pi 0d_{\frac{5}{2}}}\right]_{0^+} |\mathrm{CORE}\rangle. \tag{81}$$

The Final state equation

$$|f\rangle = |^{18}\mathrm{F}, 1^{+}\rangle_{gs} = \frac{1}{\sqrt{2}}\left[c^{\dagger}_{\pi 0\mathrm{d}_{\frac{5}{2}}} c^{\dagger}_{\nu 0\mathrm{d}_{\frac{5}{2}}}\right]_{1^{+}} |\mathrm{CORE}\rangle.$$

Using eq. (65), the amplitude of the Gamow-Teller decay transition

$$\mathcal{M}^{(+)}_{L=1}\left(\pi 0d_{\frac{5}{2}}\pi 0d_{\frac{5}{2}}\, J_i = 0^{+} \rightarrow \pi 0d_{\frac{5}{2}}\,\nu 0d_{\frac{5}{2}}\, J_f = 1^{+}\right)$$

$$= \sqrt{3} \times 1 \times \sqrt{3} \times \frac{1}{\sqrt{2}} \times (-1)^{1} \times 2\left[\sqrt{\frac{14}{5}} \times \left(\frac{1}{3\sqrt{2}}\right)\right], \quad (82)$$

$$= -\sqrt{\frac{14}{5}}.$$

Noting that

$$\mathcal{M}^{(+)}_{L=0}\left(\pi 0d_{\frac{5}{2}}\pi 0d_{\frac{5}{2}}\, J_i = 0^{+} \rightarrow \pi 0d_{\frac{5}{2}}\,\nu 0d_{\frac{5}{2}}\, J_f = 1^{+}\right) = 0,$$

The transition yields the ground state ^{18}F. Using eq. (9), we obtain the reduced Gamow-Teller transition amplitude

$$B_{GT} = \frac{(1.25)^{2}}{2 \times 0 + 1}\left|-\sqrt{\frac{14}{5}}\right|^{2} = \frac{25}{1} \times \left|-\sqrt{\frac{14}{5}}\right|^{2} = 4.375, \quad (83)$$

and $B_F = 0$. Thus the half-life times the phase space factor becomes

$$f_0 t_{\frac{1}{2}} = \frac{\kappa}{(B_F + B_{GT})} = \frac{6147\ \mathrm{s}}{(0 + 4.375)} = 1405.03\ \mathrm{s}. \quad (84)$$

From eq. (12) We find,

$$logft = log(1405.03) = 3.15, \quad (85)$$

The experimental value for $logft_{\mathrm{exp}}$ = 3.1 which makes the deviations

$$error = \frac{3.15 - 3.1}{3.1} \times 100 = 1.6\%,$$

which is an excellent agreement between theory and experiment.

Let us consider the Fermi transition

$$\left|^{18}\mathrm{Ne}, \pi 0d_{\frac{5}{2}}\pi 0d_{\frac{5}{2}}, 0^{+}\right\rangle_{gs} \rightarrow \left|^{18}\mathrm{F}, \pi 0d_{\frac{5}{2}}\,\nu 0d_{\frac{5}{2}}, J_f = 0^{+}\right\rangle_{1.042\mathrm{MeV}},$$

corresponds to forming ^{18}F at the first excited state, as shown in fig. (10). From eq (65), the Fermi transition dictates that $J_i = J_f$ according to the selection rule. The Fermi transition amplitude becomes,

$$\mathcal{M}_{L=0}^{(+)}\left(\pi 0d_{\frac{5}{2}}\pi 0d_{\frac{5}{2}}\, J_i = 0^+ \rightarrow \pi 0d_{\frac{5}{2}}\, \nu 0d_{\frac{5}{2}}\, J_f = 0^+\right)$$
$$= \mathcal{N}_{p_i p_i'}\begin{bmatrix}(-1)^{\frac{5}{2}+\frac{5}{2}+0+0}\left(-\frac{1}{\sqrt{6}}\right)\mathcal{M}_L\left(\pi 0d_{\frac{5}{2}}\, \nu 0d_{\frac{5}{2}}\right)+ \\ (-1)^{\frac{5}{2}+\frac{5}{2}+0+0+0}\left(-\frac{1}{\sqrt{6}}\right)\mathcal{M}_L\left(\pi 0d_{\frac{5}{2}}\, \nu 0d_{\frac{5}{2}}\right)\end{bmatrix}$$

According to equation (20), The Fermi single-particle matrix becomes

$$\mathcal{M}_L\left(\pi 0d_{\frac{5}{2}}\, \nu 0d_{\frac{5}{2}}\right) = \sqrt{6}\,,$$

Using. eq (65) the amplitude of the Fermi transition

$$\mathcal{M}_{L=0}^{(+)}\left(\pi 0d_{\frac{5}{2}}\pi 0d_{\frac{5}{2}}\, J_i = 0^+ \rightarrow \pi 0d_{\frac{5}{2}}\nu 0d_{\frac{5}{2}}\, J_f = 0^+\right) = 1 \times 1 \times 1 \times \frac{1}{\sqrt{2}} \times$$
$$(-1)^1 \times 2\left[\sqrt{6} \times \left(-\frac{1}{\sqrt{6}}\right)\right] = \sqrt{2}\,,$$

This transition constitutes the transition to the first excited state of ^{18}F. The transitions to the final nuclear angular momentum states $J_f = 2^+, 3^+, 4^+, 5^+$ are not allowed due to selection rule imposed by the 6-*j* symbol in eq. (65). The reduced Fermi transition amplitude is obtained using eq. (8)

$$B_F = \frac{(1)^2}{2\times 0+1}\left|\sqrt{2}\right|^2 = 1 \times \left|\sqrt{2}\right|^2 = 2, \tag{86}$$

The half-life times the phase space factor becomes

$$f_0 t_{\frac{1}{2}} = \frac{\kappa}{(B_F + B_{GT})} = \frac{6147\text{ s}}{(2+0)} = 3073.5\text{ s}.$$

The *logft* value is thus,

$$logft = log(3073.5) = 3.5\,, \tag{87}$$

The experimental value of *logft* = 3.5 [32], the calculated *logft* values agrees exactly with the experiment values for the decay (78) and (79).

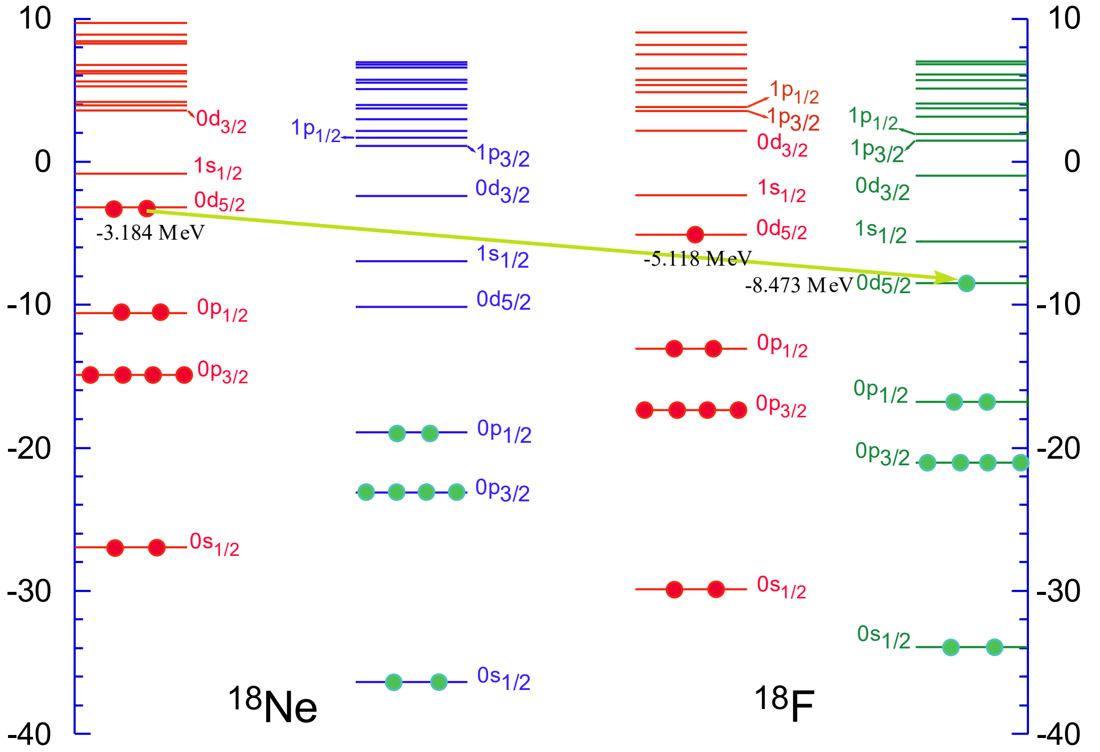

Figure 6: The First transition of ^{18}Ne to ^{18}F. The change in energy is ΔE = 5.28 MeV. Allowed by Fermi and Gamow-Teller transitions.

2- The second transition

$$\left|{}^{18}\mathrm{Ne}, \pi 0d_{\frac{5}{2}}\, \pi 0d_{\frac{5}{2}}, 0^{+}\right\rangle \rightarrow \left|{}^{18}\mathrm{F}, \pi 1s_{\frac{1}{2}}\, \nu 1s_{\frac{1}{2}}, J_f = 0^{+}, 1^{+}\right\rangle. \tag{88}$$

This transition is depicted in fig. (7). The amplitude of the transition

$$\mathcal{M}^{(+)}_{L=0.1}\left(\pi 0d_{\frac{5}{2}}\pi 0d_{\frac{5}{2}}\, J_i = 0^{+} \rightarrow \pi 1s_{\frac{1}{2}}\, \nu 1s_{\frac{1}{2}}\, J_f = 0^{+}\text{or } 1^{+}\right) = 0\ . \tag{89}$$

$\mathcal{M}_{GT} = 0, \mathcal{M}_{F} = 0$ i.e. the transitions are inhabited for Fermi and the Gamow-Teller by single particle matrix.

3- The third transition

$$\left|{}^{18}\mathrm{Ne}, \pi 0d_{\frac{5}{2}}\pi 0d_{\frac{5}{2}}, J_i = 0^{+}\right\rangle \rightarrow \left|{}^{18}\mathrm{F}, \pi 0d_{\frac{5}{2}}\, \nu 0d_{\frac{3}{2}}, J_f = 1^{+}, 2^{+}, 3^{+}, 4^{+}\right\rangle,$$

is depicted in fig. (8). Using eq (65) for all possible $J_f = 1^+, 2^+, 3^+$, and 4^+, only $J_f = 1^+$ contributes since the 6-j symbol matrix yields zero for $J_f > 1^+$. Note that this transition requires energy of 2.214 MeV of the Q-value. Part of the remaining energy 4.44 MeV – 2.214 MeV = 2.226 MeV is consumed as

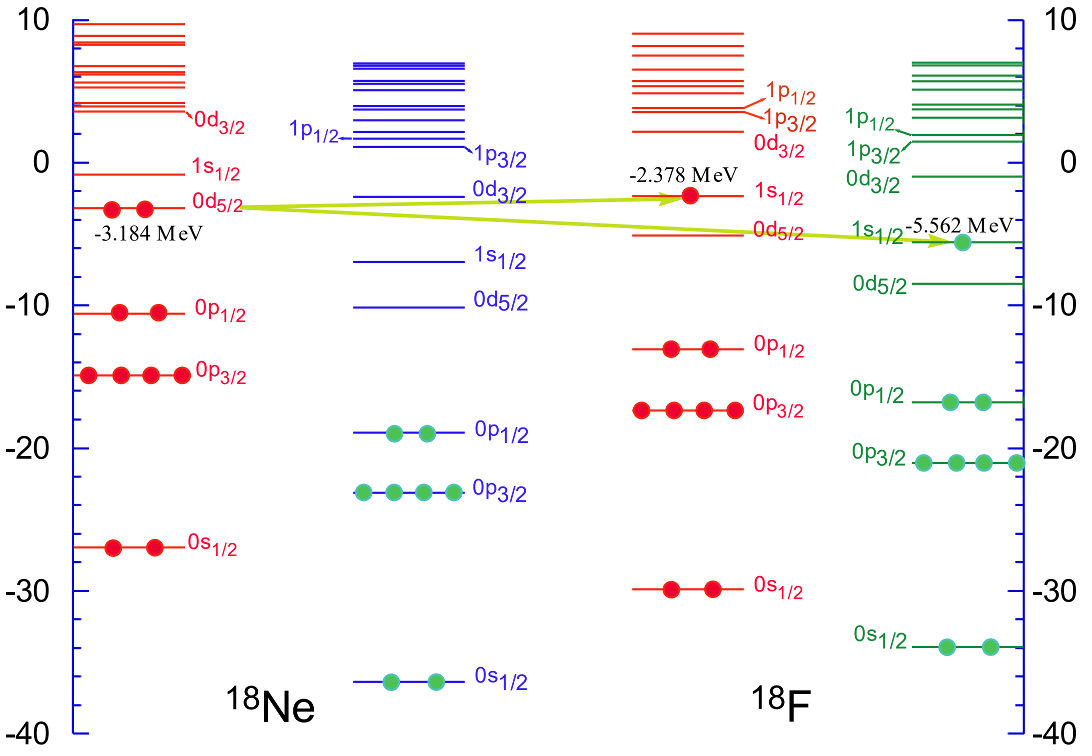

Figure7: The second transition of ^{18}Ne to ^{18}F. The change in energy is $\Delta E = 2.378$MeV. The Fermi and Gamow-Teller amplitudes vanish according since the single-particle matrix does not allow the transition.

an excitation for ^{18}F, presumably the 3.721 MeV 1^+ state, shown in fig. (10). The initial state equation

$$|i\rangle = |^{18}\mathrm{Ne}, 0^+\rangle_{gs} = \frac{1}{\sqrt{2}}\left[c^\dagger_{\pi 0d_{\frac{5}{2}}} c^\dagger_{\pi 0d_{\frac{5}{2}}}\right]_{0^+} |CORE\rangle. \tag{90}$$

The Final state equation

$$|f\rangle = |^{18}\mathrm{F}, 1^+\rangle_{3.721\mathrm{MeV}} = \frac{1}{\sqrt{2}}\left[c^\dagger_{\pi 0d_{\frac{5}{2}}} c^\dagger_{\nu 0d_{\frac{3}{2}}}\right]_{1^+} |CORE\rangle, \tag{91}$$

We obtain the amplitude of the transition for Gamow-Teller decay using. eq (65),

$$\mathcal{M}^{(+)}_{L=1}\left(\pi 0d_{\frac{5}{2}}\pi 0d_{\frac{5}{2}}, J_i = 0^+ \rightarrow \pi 0d_{\frac{5}{2}}\,\nu\, 0d_{\frac{3}{2}},\, J_f = 1^+\right) =$$
$$\hat{L}\sqrt{2\times 0+1}\,\sqrt{2\times 1+1}\,\mathcal{N}_{p_i p_i'}\left[(-1)^{\frac{3}{2}+\frac{5}{2}+1+L}\begin{Bmatrix} 0 & 1 & L \\ \frac{3}{2} & \frac{5}{2} & \frac{5}{2}\end{Bmatrix}\mathcal{M}_L\right.$$
$$\left.\left(\pi 0d_{\frac{5}{2}}\,\nu 0d_{\frac{3}{2}}\right) + (-1)^{\frac{5}{2}+\frac{3}{2}+0+1+L}\begin{Bmatrix} 0 & 1 & L \\ \frac{3}{2} & \frac{5}{2} & \frac{5}{2}\end{Bmatrix}\mathcal{M}_L\left(\pi 0d_{\frac{5}{2}}\,\nu 0d_{\frac{3}{2}}\right)\right].$$

The Gamow-Teller transition amplitude becomes

$$\mathcal{M}_{L=1}^{(+)}\left(\pi 0d_{\frac{5}{2}}\pi 0d_{\frac{5}{2}}\, J_i = 0^+ \rightarrow \pi 0d_{\frac{5}{2}}\, \nu\, 0d_{\frac{3}{2}}\, J_f = 1^+\right) = \frac{4}{\sqrt{5}}\,. \tag{92}$$

We end up with

$$\mathcal{M}_{GT} = \frac{4}{\sqrt{5}} \text{ and } \mathcal{M}_F = 0.$$

The transition is not allowed for Fermi due to the single particle matrix element which prohibits the Fermi transition from $\pi 0d_{\frac{5}{2}} \rightarrow \nu\, 0d_{\frac{3}{2}}$ since $j_i \neq j_f$ in eq. (20).

Using the eq (9). We find the reduced for the Gamow-Teller transition,

$$B_{GT} = \frac{(1.25)^2}{2\times 0+1}\left|\frac{4}{\sqrt{5}}\right|^2 = \frac{25}{1}\times\left|\frac{4}{\sqrt{5}}\right|^2 = 5.0\,, \tag{93}$$

then we find the half-life to phase space factor

$$f_0 t_{\frac{1}{2}} = \frac{\kappa}{(B_F+B_{GT})} = \frac{6147\ \mathrm{s}}{(0+5)} = 1229.4\ \mathrm{s.}\ , \tag{94}$$

The *logft* value

$$logft = \log(1229.4) = 3.1\,. \tag{95}$$

No experimental value is available for such a transition. This transition is suppressed experimentally due to the relatively high excitation of the ^{18}F (3.721 MeV) compared to the Q-value of the decay.

4- The Fourth transition

$$\left|{}^{18}Ne, \pi 0d_{\frac{5}{2}}\, \pi 0d_{\frac{5}{2}}, 0^+\right\rangle \rightarrow \left|{}^{18}\mathrm{F}, \pi 0d_{\frac{5}{2}}\, \nu 1s_{\frac{1}{2}}\,, J_f = 2^+, 3^+\right\rangle, \tag{96}$$

is depicted in fig. (9). According to eq (65) the amplitude of the transitions to $J_f = 2^+, 3^+$states are prohibited by both the single particle matrix and the 6-j symbol matrix. Thus

$$\mathcal{M}_{L}^{(+)}\left(\pi 0d_{\frac{5}{2}}\pi 0d_{\frac{5}{2}}\, J_i = 0^+ \rightarrow \pi 0d_{\frac{5}{2}}\, \nu 1s_{\frac{1}{2}}\ J_f = 2^+, 3^+\right) = 0\,. \tag{97}$$

Fig. (10) summarizes all possible transitions for decays (78) and (79). Note that decay (^{18}Ne, 0.00 MeV, 0^+) to (^{18}F, 1.081 MeV, 0^-) is not allowed due to parity conservation. The Fermi transitions do not violate parity, unlike, Gamow-Teller transitions which do not conserve parity. Transitions to energy levels higher than or equal to 1.701 MeV of ^{18}F are theoretically allowed because they involve Gamow-Teller transitions. However, they are forbidden according to the single-particle amplitude since they involve transitions from d-subshells to p- and s-subshells. However, the s-d shell mixing gives rise to small probability of such transitions as discussed next.

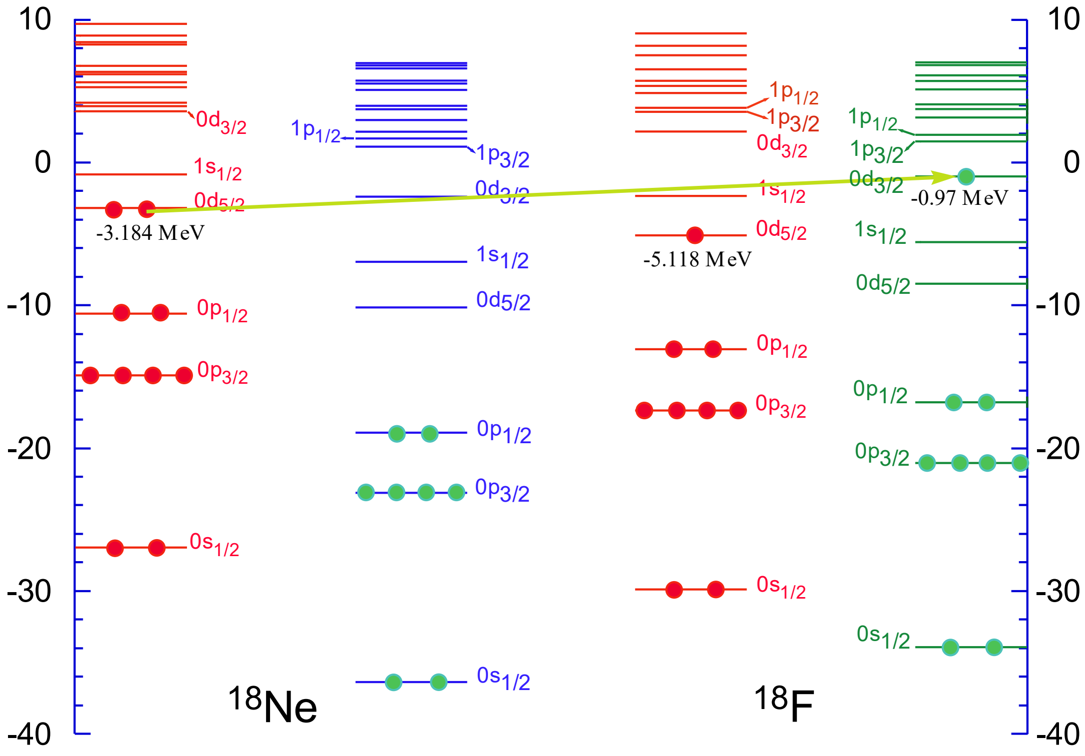

Figure8: The third transition of ^{18}Ne to ^{18}F. The change in energy is ΔE = 2.214 MeV. According to eq. (20), the Fermi transition is not allowed since $j_i = 5/2 \neq j_f = 3/2$. This transition from ^{18}F at state (1^+, 3.721 MeV).

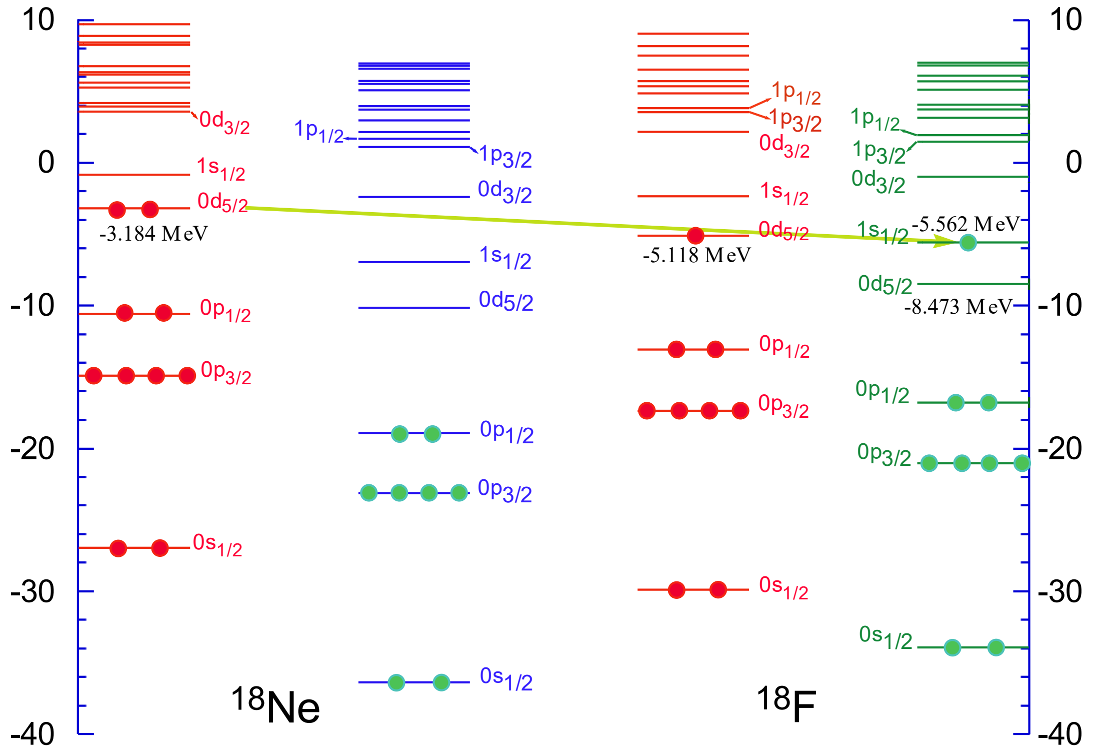

Figure9: The fourth transition of ^{18}Ne to ^{18}F. The change in energy when transitioning a proton (π) → proton (π) $\Delta E = 1.934$ MeV and the change in energy when transitioning a proton (π) → neutron (ν) $\Delta E = 2.378$ MeV. This transition is prohibited by two selection rules of the single-particle transition amplitude and 6j-symbol.

3.4 s-d Shells Mixing of ^{18}F

We can assume configuration mixing for s- and d-shell in the 1^+ state of ^{18}F. This is expected because the mean filed states $\left|^{18}\mathrm{F}, \pi 0d_{\frac{5}{2}}\, \nu 0d_{\frac{5}{2}}, 1^+\right\rangle$ and $\left|^{18}\mathrm{F}, \pi 1s_{\frac{1}{2}}\, \nu 1s_{\frac{1}{2}}, 1^+\right\rangle$ can be mixed due to the narrow energy gap, as depicted by fig. (11). The mixing can be expressed by two orthonormal states

$$|^{18}\mathrm{F}\,, 1^+\rangle_1 = A\left|\pi 0d_{\frac{5}{2}}\, \nu 0d_{\frac{5}{2}}\,, 1^+\right\rangle + B\left|\pi 1s_{\frac{1}{2}}\, \nu 1s_{\frac{1}{2}}, 1^+\right\rangle, \tag{98}$$

$$|^{18}\mathrm{F}\,, 1^+\rangle_2 = -B\left|\pi 0d_{\frac{5}{2}}\, \nu 0d_{\frac{5}{2}}\,, 1^+\right\rangle + A\left|\pi 1s_{\frac{1}{2}}\, \nu 1s_{\frac{1}{2}}\,, 1^+\right\rangle, \tag{99}$$

$${}_1\langle 1^{+\,18}\mathrm{F}, |1^+, {}^{18}\mathrm{F}\rangle_1 = {}_2\langle 1^{+\,18}\mathrm{F}, |1^+, {}^{18}\mathrm{F}\rangle_2 = A^2 + B^2 = 1 \text{ (normalization)}$$

$${}_1\langle 1^{+\,18}\mathrm{F}, |1^+, {}^{18}\mathrm{F}\rangle_2 = 0 - AB + BA = 0 \text{ (orthogonality)}.$$

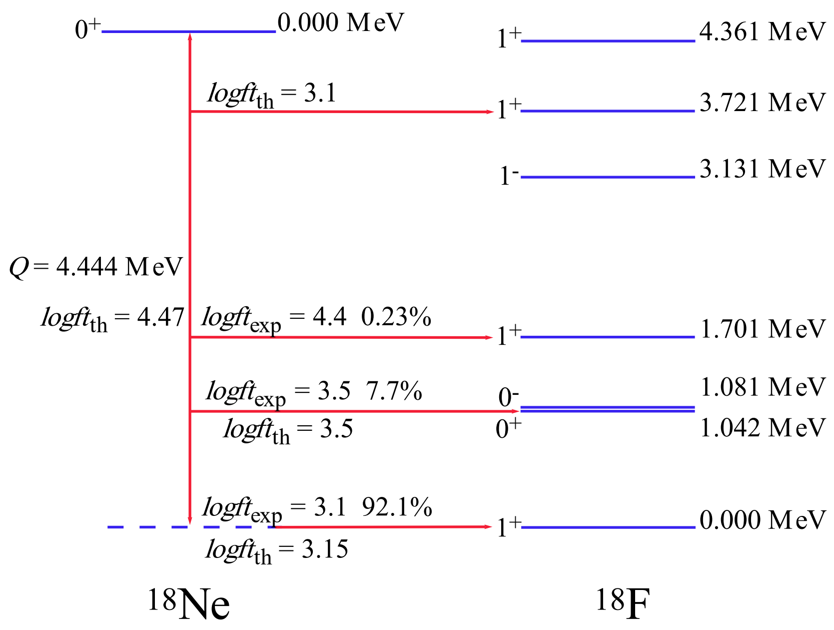

Figure10: All possible transitions for the β^+/EC decays (78) and (79). The figure shows the calculated *logft* values as well as the experimental *logft* values plus the branching ratios of the decays.

Since the transition to s-state is not allowed, we expect that $B \ll A$. The vales of A and B is determined by experiment. Both states are due to GT transitions. We modify our result such that the nuclear Gamow-Teller transition amplitude for the first state

$$\mathcal{M}_{GT}({}^{18}\mathrm{Ne}, 0^+ \to 1^+, {}^{18}F)_1 = -\sqrt{\frac{14}{5}}A\,, \tag{100}$$

and the nuclear Gamow-Teller transition amplitude for the second state

$$\mathcal{M}_{GT}({}^{18}\mathrm{Ne}, 0^+ \to 1^+, {}^{18}\mathrm{F})_2 = -\sqrt{\frac{14}{5}}\,(-B) = \sqrt{\frac{14}{5}}\,B. \tag{101}$$

Hence, the reduced Gamow-Teller transition amplitude for the first and the second state are

$$B_{GT}(0^+_{gs} \to 1^+)_1 = \tfrac{14}{5}{g_A}^2A^2, \tag{102}$$

and

$$B_{GT}(0^+_{gs} \to 1^+)_2 = \frac{14}{5} g_A{}^2 B^2, \tag{103}$$

`are $B_{GT_1} = 4.88$ and $B_{GT_2} = 0.245$ [38]. Dividing eq. (102) over eq. (103) we obtain

$$\frac{B_{GT}(0^+_{gs} \to 1^+)_1}{B_{GT}(0^+_{gs} \to 1^+)_2} = \frac{A^2}{B^2} = \frac{4.88}{0.245} = 19.9,$$

make use of the normalization condition, we obtain the values of the square of mixing amplitudes, to be $A^2 = 0.952$ and $B^2 = 0.048$.

Using eq. (98), the first initial state is thus,

$$|i\rangle_1 = |^{18}\mathrm{F}, 1^+\rangle_1 = 0.98 \left|\pi 0d_{\frac{5}{2}}\, \nu 0d_{\frac{5}{2}}, 1^+\right\rangle + 0.22 \left|\pi 1s_{\frac{1}{2}}\, \nu 1s_{\frac{1}{2}}, 1^+\right\rangle, \tag{104}$$

whereas, using eq. (99) the second initial state is

$$|i\rangle_2 = |^{18}F, 1^+\rangle_2 = -0.22 \left|\pi 0d_{\frac{5}{2}}\nu\, 0d_{\frac{5}{2}}, 1^+\right\rangle + 0.98 \left|\pi 1s_{\frac{1}{2}}\, \nu 1s_{\frac{1}{2}}, 1^+\right\rangle. \tag{105}$$

Note that the decay of ^{18}Ne $(0^+)_{gs}$ to ^{18}F $(1^+)_2$ (the second decay of ^{18}Ne) is not allowed as indicated in eq. (88). This is reflected upon the smallness of the value of B^2. However, this mixing scheme can affect the decay of ^{18}F to ^{18}O, as shown next.

Modification is executed to the 2nd transition (88) to account for the small amplitude in eq. (103). This transition forms ^{18}F at state (1+, 1.701 MeV). We can calculate the reduced amplitude to be

$$\mathcal{M}_{GT}(^{18}\mathrm{Ne}, 0^+_{\mathrm{gs}} \to {}^{18}\mathrm{F}, 1^+_{1.7})_2 = \sqrt{\frac{14}{5}}\, B. \tag{106}$$

The reduced transition amplitudes are

$$B_{GT} = \frac{(1.25)^2}{2 \times 0 + 1} \left| \sqrt{\frac{14}{5}}\, B \right|^2 = \frac{(1.25)^2}{1} \times \frac{14}{5} \times 0.048 = 0.21, \tag{107}$$

where as $B_F = 0$. This corresponds to $f_0 t_{1/2}$ value

$$f_0 t_{\frac{1}{2}} = \frac{\kappa}{(B_F + B_{GT})} = \frac{6147}{(0 + 0.21)} = 29271.4, \tag{108}$$

where the *logft* value is

$$logft = log(29271.4) = 4.47\,. \tag{109}$$

The experimental value is 4.4 which makes the deviations

$$error\ = \frac{4.47 - 4.4}{4.4} \times 100 = 0.16\%,$$

in an excellent agreement between theory and experiment. The agreement in this case is due to the fact that theory is tailored to experiment when use the experimental reduced amplitudes derived from experimental decay width [32].

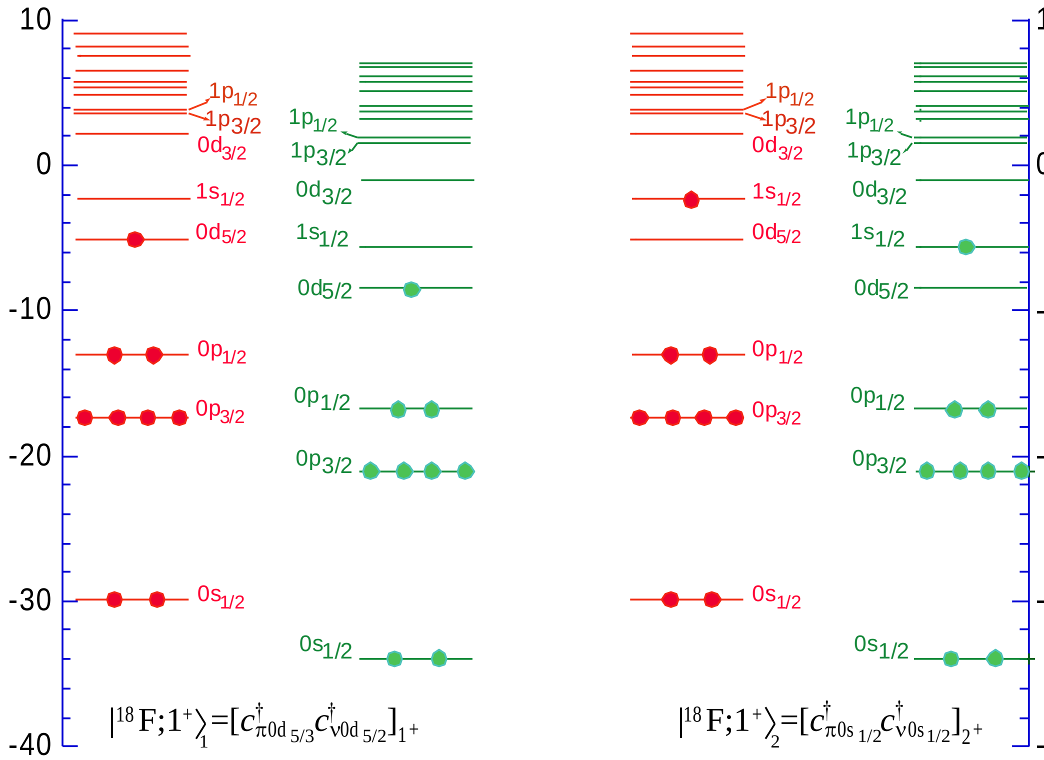

Figure 11: The s-d shell mixing of the ground state of ^{18}F. The state equations are given in eqs. (104)-(105).

3.5 The β^+-decay of ^{18}F

The equation of decay for β^+ of ^{18}F is:

$$ {}^{18}_{9}\mathrm{F}_9 \rightarrow {}^{18}_{8}\mathrm{O}_{10} + \beta^+ + \nu_e, \tag{110} $$

whereas for EC, the equation of the decay is:

$$ {}^{18}_{9}\mathrm{F}_9 + e \rightarrow {}^{18}_{8}\mathrm{O}_{10} + \nu_e, \tag{111} $$

With the Q-value $Q_{\mathrm{EC}} = 1.6559$ MeV [32]. Not that $^{18}\mathrm{O}$ is formed at the ground state since the Q-value is smaller than the first excited state of $^{18}\mathrm{O}$ (1.98 MeV). Make use equation (66), one calculates the transition amplitudes using the two-particle and two-hole theory.

The only transition is ground state $^{18}\mathrm{F}$ ($J_i = 1^+$) to ground state of $^{18}\mathrm{O}$ ($J_f = 0^+$).

$$ \left|{}^{18}\mathrm{F}, \pi\, 0d_{\frac{5}{2}}\, \nu 0d_{\frac{5}{2}}, J_i = 1^+\right\rangle_{gs} \rightarrow \left|{}^{18}\mathrm{O}, \nu 0d_{\frac{5}{2}}\, \nu 0d_{\frac{5}{2}}, J_f = 0^+\right\rangle_{gs}. $$

The initial state equation

$$ |i\rangle = |{}^{18}\mathrm{F}, 1^+\rangle_{gs} = \frac{1}{\sqrt{2}}\left[c^{\dagger}_{\pi 0d_{\frac{5}{2}}} c^{\dagger}_{\nu 0d_{\frac{5}{2}}}\right]_{1^+} |CORE\rangle. \tag{112} $$

The Final state equation

$$ |f\rangle = |{}^{18}\mathrm{O}, 0^+\rangle_{gs} = \frac{1}{\sqrt{2}}\left[c^{\dagger}_{\nu 0d_{\frac{5}{2}}} c^{\dagger}_{\nu 0d_{\frac{5}{2}}}\right]_{0^+} |CORE\rangle. \tag{113} $$

The transition is from proton-neutron to neutron-neutron; thus, we use. eq (66) to find the amplitude of the transition of the Gamow-Teller decay,

$$ \mathcal{M}^{(+)}_{L=1}\left(\pi 0d_{\frac{5}{2}}\nu 0d_{\frac{5}{2}} J_i = 1^+ \rightarrow \nu 0d_{\frac{5}{2}}\nu 0d_{\frac{5}{2}} J_f = 0^+\right) = \sqrt{3} \times 1 \times \sqrt{3} \times \frac{1}{\sqrt{2}} \times (-1)^7 \times \left[\sqrt{\frac{14}{5}} \times \frac{1}{3\sqrt{2}}\right] = -\sqrt{\frac{14}{5}}\ . \tag{114} $$

We end up with

$$ \mathcal{M}_{GT} = -\sqrt{\frac{14}{5}}. $$

The reduced Gamow-Teller transition amplitudes is calculated using eq. (9),

$$B_{GT} = \frac{(1.25)^2}{2\times 1+1}\left|-\sqrt{\frac{14}{5}}\right|^2 = (1.25)^2\frac{14}{15} = 1.46, \tag{115}$$

The half-life to phase space factor becomes,

$$f_0 t_{\frac{1}{2}} = \frac{6147\ \text{s}}{(0+1.46)} = 4215.09\ \text{s}, \tag{116}$$

corresponds to *logft* value

$$logft = 3.62\,. \tag{117}$$

The experimental value is 3.6 [32]. The error of $logft$ is:

$$\text{error} = \frac{3.6-3.62}{3.6}\times 100 = 0.55\%.$$

The deviation is very small. Once again, the two-particle two-hole theory successfully describes the strength function for the decays (110) and (111).

The reader must notice that the initial state of ^{18}F in eq. (112) is in fact the $|^{18}\text{F}\,,1^+\rangle_1$ given in eq. (104). In this case the reduced amplitude (115) is composed of two terms, one term has A^2 and the other one has B^2. The normalization condition $A^2+B^2=1$ makes the value of the reduced amplitude (115) unaltered. Thus, the mixing does not change the final value of (117).

3.6 The β^+-decay of ^{42}Sc

The equation of decay for β^+ is:

$$^{42}_{21}\text{Sc}_{21} \rightarrow {}^{42}_{22}\text{Ca}_{20} + \beta^+ + \nu_e, \tag{118}$$

whereas for EC, the equation of the decay is:

$$^{42}_{21}\text{Sc}_{21} + e \rightarrow {}^{42}_{22}\text{Ca}_{20} + \nu_e. \tag{119}$$

The Q-value $Q_{\text{EC}} = 6.42629$ MeV [32].

1. First transition, depicted in fig. (12), is a Fermi transition from proton-neutron to neutron-neutron state. Thus, we use eq. (66) to calculate the transition amplitude

$$\mathcal{M}^{(+)}_{L=0}\left(\pi 0f_{\frac{7}{2}}\nu 0f_{\frac{7}{2}}J_i = 0^+ \rightarrow \nu 0f_{\frac{7}{2}}\nu 0f_{\frac{7}{2}}J_f = 0^+\right) = \sqrt{2}\,,$$

Using eq. (8), the reduced amplitude for the Fermi transition,

$$B_F = \frac{g_V^2}{2J_i+1}\left|\mathcal{M}_f\right|^2 = \frac{(1.0)^2}{2\times0+1}\left|\sqrt{2}\right|^2 = 2, \tag{120}$$

The half-life of phase space factor to be

$$f_0 t_{\frac{1}{2}} = \frac{\kappa}{(B_F+B_{GT})} = \frac{6147s}{(2+0)} = 3073.5\text{ s}, \tag{121}$$

Hence the $logft$ is

$$logft = log(3073.5) = 3.487. \tag{122}$$

The experimental value is 3.5 [32]. The error of $logft$ is:

$$\text{error} = \frac{3.5-3.487}{3.5}\times 100 = 0.37\%.$$

The calculated *logft* value of the EC/β^+- decays (118) and (119) of transition 1, agrees very well with the experimental value.

2. The second transition, depicted in fig. (13), is a Gamow-Teller. Using eq (66) the value of the amplitude is

$$\mathcal{M}_{L=1}^{(+)}\left(\pi 0f_{\frac{7}{2}}\nu 0f_{\frac{7}{2}}J_i = 0^+ \rightarrow \nu 0f_{\frac{7}{2}}\nu 0f_{\frac{5}{2}}J_f = 1^+\right) = 2\sqrt{\frac{3}{7}},$$

Using eq (9) the reduced amplitude for the Gamow-Teller transition,

$$B_{GT} = \frac{(1.25)^2}{2\times0+1}\left|2\sqrt{\frac{3}{7}}\right|^2 = 2.678. \tag{123}$$

The half-life to phase space factor becomes

$$f_0 t_{\frac{1}{2}} = \frac{\kappa}{(B_F+B_{GT})} = \frac{6147\text{ s}}{(0+2.678)} = 2295.369\text{ s}, \tag{124}$$

The $logft$ is,

$$logft = log(2295.369) = 3.355, \tag{125}$$

According to table (1), the transition is super allowed, however, it is not detected experimentally since it requires 2.1 MeV to occur, unlike the first transition which releases 5.25 MeV (close the Q-value of the decay).

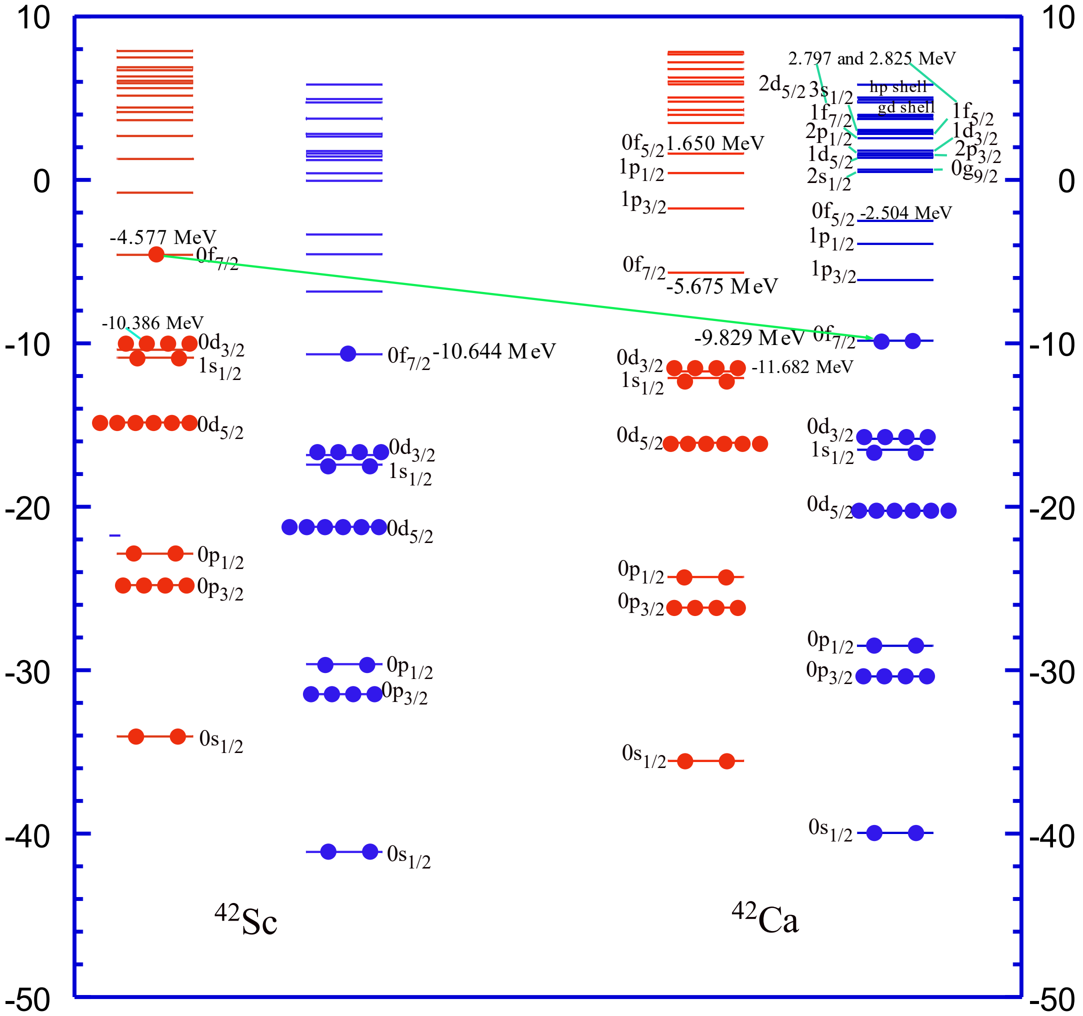

Figure 12: The first transition of ^{42}Sc to ^{42}Ca. The change in energy is $\Delta E = 5.252$ MeV.

3. Third transition from ^{42}Sc 7^+, 0.616 MeV metastable state to ^{42}Ca 6^+, 3.189 MeV excited state. Using. eq (66) the transition amplitude is

$$\mathcal{M}_L^{(+)}\left(\pi 0f_{\frac{7}{2}}\nu 0f_{\frac{7}{2}} J_i = 7^+ \rightarrow \nu 0f_{\frac{7}{2}}\nu 0f_{\frac{7}{2}} J_f = 6^+\right) = -\sqrt{\frac{30}{7}}$$

The transition amplitude is for the Gamow-Teller decay. Using the eq (9), the reduced amplitude for the Gamow-Teller transition,

$$B_{GT} = \frac{(1.25)^2}{2\times 7+1}\left|-\sqrt{\frac{30}{7}}\right|^2 = 0.446\,, \qquad (126)$$

The half-life to phase space factor becomes

$$f_0 t_{\frac{1}{2}} = \frac{\kappa}{(B_F + B_{GT})} = \frac{6147}{(0+0.446)} = 13782.5112\,, \quad (127)$$

The *logft* values is,

$$logft = log(2295.369) = 4.139, \quad (128)$$

The experimental value is 4.2 [32]. The error of $logft$ is:

$$\text{error} = \frac{4.2-4.139}{4.139} \times 100 = 1.47\%.$$

The *logft* value for the EC/β^+ transition 3 for the decays (118) and (119), calculated using the two-particle and hole theory, agrees very well with the experimental value.

4.Forth transition from ^{42}Sc 7^+, 0.616 MeV metastable state to ^{42}Ca 6^+, 5.62 MeV excited state. Using. eq (66), the Gamow-Teller transition amplitude is

$$\mathcal{M}^{(+)}_{L=1}\left(\pi 0f_{\frac{7}{2}} \nu 0f_{\frac{7}{2}} J_i = 7^+ \rightarrow \nu 0f_{\frac{7}{2}} \nu 0f_{\frac{5}{2}} J_f = 6^+\right) = -6\sqrt{\frac{5}{7}}\,,$$

Using eq (9), the reduced amplitude for the Gamow-Teller transition,

$$B_{GT} = \frac{(1.25)^2}{2\times7+1}\left|-6\sqrt{\frac{5}{7}}\right|^2 = 2.6785\,, \quad (129)$$

The half-life to phase space factor becomes

$$f_0 t_{\frac{1}{2}} = \frac{\kappa}{(B_F + B_{GT})} = \frac{6147\text{ s}}{(0+2.6785)} = 2294.9411\text{ s.} \quad (130)$$

And the *logft* value is

$$logft = log(2294.9411) = 3.36, \quad (131)$$

There is no experimental value for the *logft* value since this transition forms ^{42}Ca at excited state close to the Q-value of the decay.

Fig. (14) summarizes all possible transitions for decays (118) and (119).

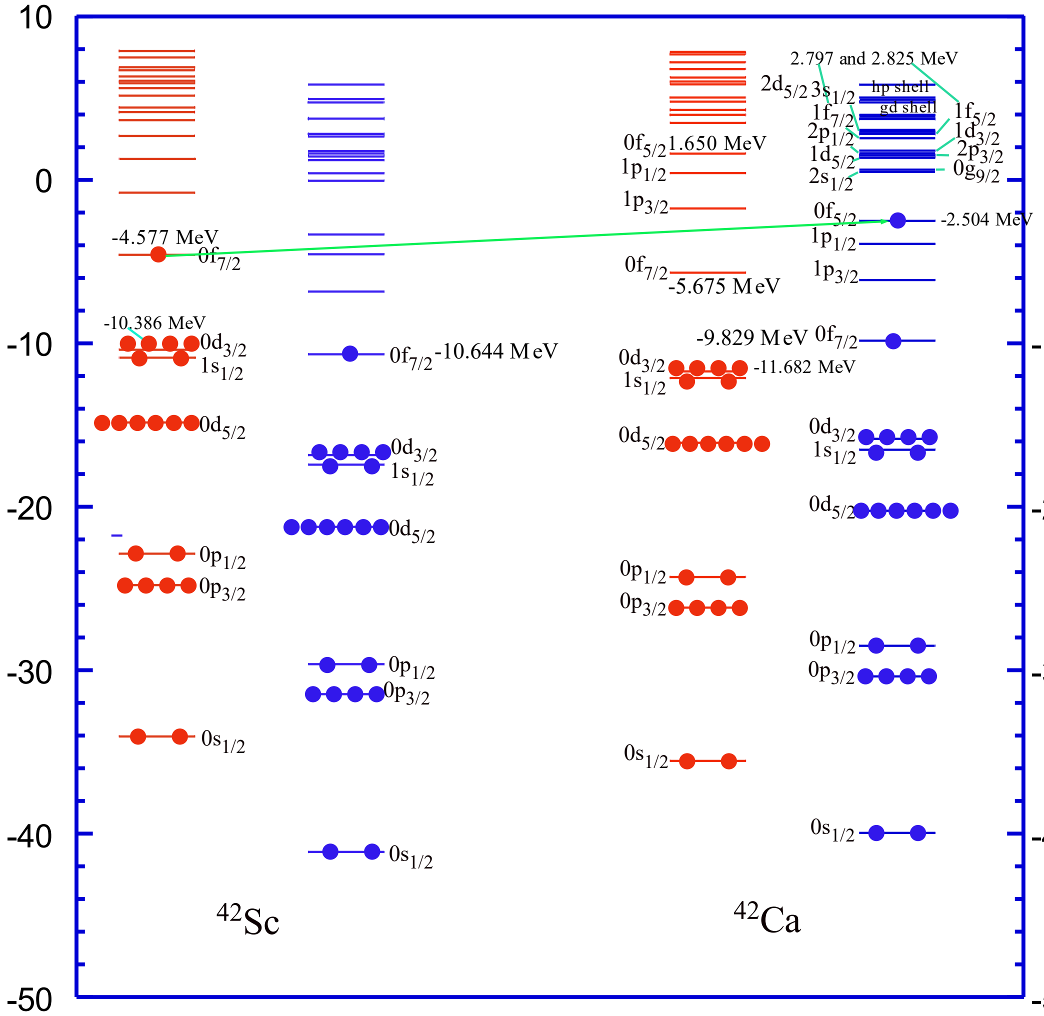

Figure 13: The second transition of ^{42}Sc to ^{42}Ca. The change in energy is $\Delta E = 2.073$ MeV. Allowed Gamow-Teller transitions.

Conclusion

In conclusion, the comprehensive analysis presented in this paper demonstrates that the two-particle theory provides a robust framework for describing Fermi and Gamow-Teller transitions across a spectrum of light to medium even-even and odd-odd nuclei. The empirical evidence and theoretical calculations align to affirm the theory's predictive power and its significant role in advancing our understanding of nuclear processes. Tables (2)-(5) summarize the calculation data

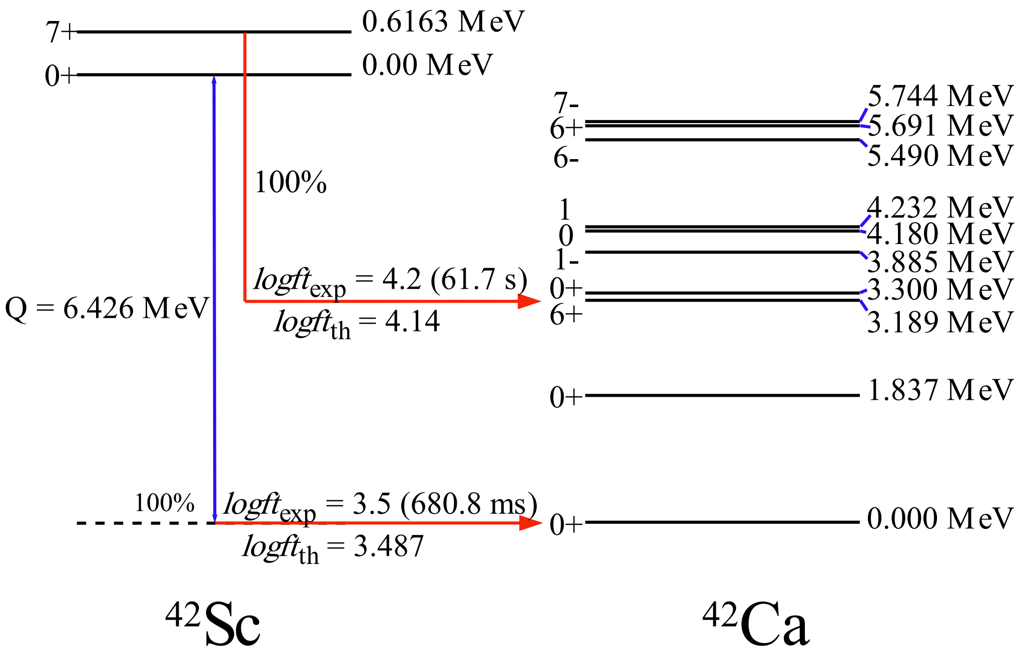

Figure 14: All possible transitions for the β^+/EC decay (118) and (119). The figure shows the calculated *logft* values as well as the experimental *logft* values plus the decay lifetime.

Table 2: Summary of the calculated β^--decay logarithm of the strength function $log\,ft$ for all allowed transitions using two-particle Theory for the decay ${}^{6}_{2}\mathrm{He}_4 \rightarrow {}^{6}_{3}\mathrm{Li}_3 + e^- + \bar{\nu}_e$ which has $Q_{\beta^-} = 3.50521$ MeV.

Single Particle Transition	SP transition Energy (MeV)	Nuclear transition	Nuclear State Energy (MeV)	Isospin	**logft**	**logft$_{exp}$**
$\boldsymbol{\nu 0p_{\frac{3}{2}} \nu 0p_{\frac{3}{2}} \rightarrow \pi 0p_{\frac{3}{2}} \nu 0p_{\frac{3}{2}}}$	2.221	$\lvert\langle 1^+ \lvert \beta_{GT} \rvert 0^+ \rangle\rvert = \sqrt{\frac{10}{3}}$	-5.975	1	3.07	2.9

Table 3: Summary of the calculated β^+/EC -decay logarithm of the strength function $log\,ft$ for all allowed transitions using two-particle Theory for the decay ${}^{18}\mathrm{Ne} \rightarrow {}^{18}\mathrm{F} + \beta^+ + \nu_e {}^{18}\mathrm{Ne} + e \rightarrow {}^{18}\mathrm{F} + \nu_e$ or which has $Q_{EC} = 4.44 MeV$.

Single Particle Transition	SP transition Energy (MeV)	Nuclear transition	Nuclear state energy (MeV)	Isospin	**logft**	**logft$_{exp}$**
$\boldsymbol{\pi 0d_{\frac{5}{2}}\pi 0d_{\frac{5}{2}} \to \pi 0d_{\frac{5}{2}}\nu 0d_{\frac{5}{2}}}$	5.289	$\lvert\langle 1^+\lvert\beta_{GT}\rvert 0^+\rangle\rvert=-\sqrt{\frac{14}{5}}$	−8.473	1	3.15	3.1
$\boldsymbol{\pi 0d_{\frac{5}{2}}\pi 0d_{\frac{5}{2}} \to \pi 0d_{\frac{5}{2}}\nu 0d_{\frac{5}{2}}}$	5.289	$\lvert\langle 0^+\lvert\beta_F\rvert 0^+\rangle\rvert=\sqrt{2}$	−8.473	1	3.5	3.5
$\boldsymbol{\pi 0d_{\frac{5}{2}}\pi 0d_{\frac{5}{2}} \to \pi 1s_{\frac{1}{2}}\nu 1s_{\frac{1}{2}}}$	2.378	$\lvert\langle 0^+\lvert\beta_{GT}\rvert 0^+\rangle\rvert=0$	−5.562	1	0	_
$\boldsymbol{\pi 0d_{\frac{5}{2}}\pi 0d_{\frac{5}{2}} \to \pi 1s_{\frac{1}{2}}\nu 1s_{\frac{1}{2}}}$	2.378	$\lvert\langle 1^+\lvert\beta_{GT}\rvert 0^+\rangle\rvert = 0$	−5.562	1	0	_
$\boldsymbol{\pi 0d_{\frac{5}{2}}\pi 0d_{\frac{5}{2}} \to \pi 0d_{\frac{5}{2}}\nu 0d_{\frac{3}{2}}}$	2.214	$\lvert\langle 1^+\lvert\beta_{GT}\rvert 0^+\rangle\rvert = \frac{4}{\sqrt{5}}$	−0.97	1	3.1	_
$\boldsymbol{\pi 0d_{\frac{5}{2}}\pi 0d_{\frac{5}{2}} \to \pi 0d_{\frac{5}{2}}\nu 1s_{\frac{1}{2}}}$	2.378	$\lvert\langle 2^+\lvert\beta_{GT}\rvert 0^+\rangle\rvert = 0$	−5.562	1	0	_

Table 4: Summary of the calculated β^+/EC -decay logarithm of the strength function $log\,ft$ for all allowed transitions using two-particle Theories the decay ${}^{18}_{9}F_9 \to {}^{18}_{8}O_{10} + \beta^+ + \nu_e$ which has $Q_{EC} = 1.6559MeV$.

Single Particle Transition	SP transition Energy (MeV)	Nuclear transition	Nuclear State Energy (MeV)	Isospin	**logft**	**logft$_{exp}$**
$\boldsymbol{\pi 0d_{\frac{5}{2}}\nu 0d_{\frac{5}{2}} \to \nu 0d_{\frac{5}{2}}\nu 0d_{\frac{5}{2}}}$	0.3241	$\lvert\langle 1^+\lvert\beta_{GT}\rvert 0^+\rangle\rvert = -\sqrt{\frac{14}{5}}$	1.98	1	3.62	3.6

Table 5: Summary of the calculated β^{+}/EC -decay logarithm of the strength function $log\, ft$ for all allowed transitions using two-particle Theory for the decay ${}^{42}_{21}\mathrm{Sc}_{21} \rightarrow {}^{42}_{22}\mathrm{Ca}_{20} + \beta^{+} + \nu_{e}$ which has $Q_{EC} = 6.42629$ MeV.

Single Particle Transition	SP transition Energy (MeV)	Nuclear transition	Nuclear state energy (MeV)	Isospin	**logft**	**logft$_{exp}$**
$\pi 0f_{\frac{7}{2}} \nu 0f_{\frac{7}{2}} \rightarrow \nu 0f_{\frac{7}{2}} \nu 0f_{\frac{7}{2}}$	5.252	$\lvert\langle 1^{+} \lvert \beta_{GT} \rvert 0^{+}\rangle\rvert=0$ $\lvert\langle 0^{+} \lvert \beta_{F} \rvert 0^{+}\rangle\rvert=\sqrt{2}$	-9.829	1	3.487	3.5
$\pi 0f_{\frac{7}{2}} \nu 0f_{\frac{7}{2}} \rightarrow \nu 0f_{\frac{7}{2}} \nu 0f_{\frac{5}{2}}$	2.073	$\lvert\langle 1^{+} \lvert \beta_{GT} \rvert 0^{+}\rangle\rvert=2\sqrt{\frac{3}{7}}$	-2.504	1	3.355	–
$\pi 0f_{\frac{7}{2}} \nu 0f_{\frac{7}{2}} \rightarrow \nu 0f_{\frac{7}{2}} \nu 0f_{\frac{7}{2}}$	2.573	$\lvert\langle 6^{+} \lvert \beta_{GT} \rvert 7^{+}\rangle\rvert=-\sqrt{\frac{30}{7}}$	3.189	0	4.139	4.2
$\pi 0f_{\frac{7}{2}} \nu 0f_{\frac{7}{2}} \rightarrow \nu 0f_{\frac{7}{2}} \nu 0f_{\frac{5}{2}}$	5.004	$\lvert\langle 6^{+} \lvert \beta_{GT} \rvert 0^{+}\rangle\rvert=-6\sqrt{\frac{5}{7}}$	5.62	1	3.36	–

Bibliography:

[1] D. Lunney, J. M. Pearson, and C. Thibault, “Recent trends in the determination of nuclear masses,” Rev. Mod. Phys**.**, **vol. 75**, pp. 1021–1082, Aug 2003.

[2] V. Tripathi, S. L. Tabor, P. F. Mantica, Y. Utsuno, P. Bender, J. Cook, C. R. Hoffman, S. Lee, T. Otsuka, J. Pereira, M. Perry, K. Pepper, J. S. Pinter, J. Stoker, A. Volya, and D. Weisshaar, "Intruder configurations in the $\alpha = 33$ isobars: ^{33}Mg and ^{33}Al," Phys. Rev. Lett., **vol. 101**, p. 142504, Oct 2008.

[3] Y.-Z. Qian and G. J. Wasserburg, "Abundances of sr, y, and zr in metal-poor stars and implications for chemical evolution in the early galaxy," The Astrophysical Journal, **vol**. 687, p. 272, Nov 2008.

[4] C. S. Wu, E. Ambler, R. W. Hayward, D. D. Hoppes, and R. P. Hudson, “Experimental test of parity conservation in beta decay,” Phys. Rev., **vol**. 105, pp. 1413–1415, Feb 1957.

[5] I. S. Towner and J. C. Hardy, "The evaluation of vud and its impact on the unitarity of the Cabibbo–Kobayashi–Maskawa quark-mixing matrix," Reports on Progress in Physics, **vol. 73**, p. 046301, Mar 2010.

[6] Z. M. Niu, H. Z. Liang, B. H. Sun, W. H. Long, and Y. F. Niu, "Predictions of nuclear β-decay half-lives with machine learning and their impact on r-process nucleosynthesis," Phys. Rev. C, **vol**. 99, p. 064307, Jun 2019.

[7] N. Gove and M. Martin, "Log-f tables for beta decay," Atomic Data and Nuclear Data Tables, **vol**. 10, no. 3, pp. 205–219, 1971.

[8] J. T. Suhonen, "Value of the axial-vector coupling strength in β and $\beta\beta$ decays: A review," Frontiers in Physics, **vol. 5**, p. 55, 2017.

[9] Civitarese, O., Hess, P. O., Hirsch, J. G., & Reboiro, M. (1999). Spontaneous and dynamical breaking of mean field symmetries in the proton-neutron quasiparticle random phase approximation and the description of double β decay transitions. Physical Review C, 59(1), 194.

[10] Péru, S., Berger, J. F., & Bortignon, P. F. (2005). Giant resonances in exotic spherical nuclei within the RPA approach with the Gogny force. The European Physical Journal A-Hadrons and Nuclei, 26, 25-32.

[11] Gambacurta, D., & Grasso, M. (2022). Quenching of Gamow-Teller strengths and two-particle–two-hole configurations. Physical Review C, 105(1), 014321.

[12] Tsunoda, Y., Otsuka, T., Shimizu, N., Honma, M., & Utsuno, Y. (2014). Novel shape evolution in exotic Ni isotopes and configuration-dependent shell structure. Physical Review C, 89(3), 031301.

[13] Itaco, N., Coraggio, L., & De Gregorio, G. (2024). Gamow-Teller decays: Probing nuclear structure and weak interactions. IL NUOVO CIMENTO, 100(361), 47.

[14] Yang, M. J., Sagawa, H., Bai, C. L., & Zhang, H. Q. (2023). Effects of two-particle–two-hole configurations and tensor force on β decay of magic nuclei. Physical Review C, 107(1), 014325.

[15] Shehadeh, B., & Al-Harbyi, M. (2023). Review of Gamow-Teller and Fermi transition strength functions. Journal of Qassim University for Science, 2(1).

[16] F. Halzen and A. D. Martin, Quarks and Leptons: An Introductory Course in Modern Particle Physics. A Wiley Interscience publication, Wiley, 1991.

[17] J. Hardy, I. Towner, V. Koslowsky, E. Hagberg, and H. Schmeing, “Super allowed $0^+ \rightarrow 0^+$nuclear β-decays: A critical survey with tests of CVC and the standard model," Nuclear Physics A, **vol. 509**, no. 3, pp. 429–460, 1990.

[18] H. Buhring, Electron Radial Wave Functions and Nuclear Beta Decay. Clarendon Oxford, 1982.

[19] J. Suhonen and J. Kostensalo, “Double β-decay and the axial strength,” Frontiers in Physics, **vol. 7**, 2019.

[20] E. P. Wigner, On the Matrices Which Reduce the Kronecker Products of Representations of S. R. Groups. Berlin, Heidelberg: Springer Berlin Heidelberg, 1993.

[21] J. Sakurai and J. Napolitano, Modern Quantum Mechanics. Cambridge, 2020.

[22] G. Racah, “Theory of complex spectra. ii,” Phys. Rev., **vol. 62**, pp. 438–462, Nov 1942.

[23] E. Fermi, “Versuch einer theorie der β-strahlen,” Zeitschrift f $\ddot{u}$r Physik, **vol**. 88, p. 161, Feb 1934

[24] G. Gamow and E. Teller, “Selection rules for the β-disintegration,” Phys. Rev., **vol.** 49, pp. 895–899, Jun 1936.

[25] H. Primakoff and S. Rosen, “Double beta decay,” Reports on Progress in Physics, **vol. 22**, pp. 121–166, jan 1959.

[26] A. de Shalit and I. Talmi, Nuclear Shell Theory. Academic, 1963.

[27] C. Wu and S. Moszkowski, Beta decay. Interscience Publishers, 1966.

[28] SHIRO YOSHIDA AND LARRY ZAMICK Annu. Rev. Nucl. Sci. 1972.22:121-164.

[29] R. Edmonds: Angular Momentum in Quantum Mechanics (Princeton University Press, Princeton 1960).

[30] D.A. Varshalovich, A.N. Moskalev, V.K. Khersonskii: Quantum Theory of Angular Momentum (World Scientific Singapore 1988).

[31] E. Merzbacher. Quantum mechanics. John Wiley and Sons, 1999.

[32] Table of Nuclides - Nuclear structure and decay data, International Atomic Energy Agency.

https://www-nds.iaea.org/relnsd/vcharthtml/VChartHTML.html.

[33] A. De-Shalit, A. d. Shalit, and I. Talmi. Nuclear shell theory. Acad. Press, 1972.

[34] D. A. Varshalovich, A. N. Moskalev, and V. K. Khersonskii. Quantum Theory of Angular Momentum. WORLD SCIENTIFIC, 1988. doi: 10.1142/0270.

[35] A. Bohr and B. R. Mottelson. Nuclear structure **Vol** 1 Single structure motion. World Scienti c, 1998.

[36] Suhonen Jouni, Kostensalo Joel, "Double β Decay and the Axial Strength", Frontiers in Physics, **vol. 7**, 2019, URL=https://www.frontiersin.org/article/10.3389/fphy.2019.00029, DOI=10.3389/fphy. 2019.00029

[37] Ruben Saakyan, "Two-Neutrino Double-Beta Decay", Annual Review of Nuclear and Particle Science, **Vol. 63**: PP 503-529, October 2013.

[38] T. Inoue, T. Sebe, H. Hagiwara, A. Arima, "The structure of the sd-shell nuclei (I). ^{18}C, ^{18}F, ^{19}O, ^{19}F and ^{20}Ne." Nuclear Physics, **Vol. 59**, Issue 1, 1964,

[39] Ha, E., Cheoun, M. K., Sagawa, H., & Colo, G. (2024). Gamow-Teller strength distributions of 18O and well-deformed nuclei 24, 26Mg by deformed QRPA. arXiv preprint arXiv:2404.03884.

[40] Tian, L., Li, W., Fang, J., & Niu, Z. (2024). An empirical formula of nuclear β-decay half-lives with the transition-strength contribution. Chinese Physics C.